

# Driver Routing and Scheduling with Synchronization Constraints

Pia Ammann<sup>a,\*</sup>, Rainer Kolisch<sup>a</sup>, Maximilian Schiffer<sup>a,b</sup>

<sup>a</sup>Technical University of Munich, TUM School of Management, Arcisstr. 21, 80333 Munich, Germany

<sup>b</sup>Munich Data Science Institute, Technical University of Munich, Walther-von-Dyck-Str. 10, 85748 Garching, Germany

*Article history:* Received 13 July 2022, Revised 16 December 2022, Revised 19 March 2023, Accepted 26 May 2023.

---

## Abstract

This paper investigates a novel type of driver routing and scheduling problem motivated by a practical application in long-distance bus networks. A key difference from other crew scheduling problems is that drivers can be exchanged between buses at arbitrary intermediate stops en route such that our problem requires additional synchronization constraints. We present a mathematical model for this problem that leverages a time-expanded multi-digraph and derive bounds for the total number of required drivers. Moreover, we develop a DBMH that converges to provably optimal solutions and apply it to a real-world case study for Flixbus, one of Europe's leading coach companies. We demonstrate that our matheuristic outperforms a standalone MIP implementation in terms of solution quality and computational time and reduces the number of required drivers by up to 56% compared to approaches currently used in practice. Our solution approach provides feasible solutions for all instances within seconds and solves instances with up to 390 locations and 70 requests optimally with an average computational time under 210 seconds. We further study the impact of driver exchanges on the total driver count and show that allowing for such exchanges leads to average savings of 42.69%.

*Keywords:* Routing, Scheduling, Synchronization, Hours of service regulations, Hybrid optimization, Destructive bounds

---

## 1. Introduction

The liberalization of the European long-distance bus market caused a rapid growth in demand for intercity coach travel in recent years, resulting in competition among numerous private coach companies. Despite the long travel duration, intercity bus transportation is generally seen as a low-cost and green alternative to traveling by train or plane. Still, passengers in this sector are susceptible to price and travel duration. In this highly competitive environment, a company only survives if it keeps operational costs at a minimum. In this context, driver wages remain a major cost-share. Also, qualified drivers constitute a scarce resource for most bus companies. Accordingly, efficient scheduling and routing that keeps the number of drivers as low as possible remains a crucial planning task.

When creating driver schedules, several legal regulations concerning steering times and rest periods apply. These regulations are particularly important for long-haul passenger transport, where the trip duration

---

\*Corresponding author

*Email address:* [pia.ammann@tum.de](mailto:pia.ammann@tum.de) (Pia Ammann)

*URL:* <http://www.om.wi.tum.de> (Pia Ammann)

often exceeds a driver’s maximum steering time without break. For customer satisfaction and to remain competitive, coach companies avoid extended travel times due to drivers taking their legal breaks while passengers are waiting. Instead, they exchange drivers such that a new, sufficiently rested driver continues the trip without any delay. The first driver can then either take a break at the stop where the exchange happened, can return to a depot, or can remain as a passenger on the bus. We refer to the latter as deadheading. Such driver exchanges can happen at regular bus stops and at any service station along or near the route. Therefore, planning driver schedules in intercity bus networks includes, besides scheduling decisions, additional routing aspects and synchronization constraints. Specifically, the underlying decision problem classifies as a routing and scheduling problem with synchronization constraints and working time regulations.

Against this background, we introduce the Driver Routing and Scheduling Problem with Multiple Synchronization Constraints (DRSPMS), which comprises the planning tasks outlined above and is of high practical relevance for operational planning in long-distance bus networks. We develop a mixed-integer program (MIP) to formulate the problem on a time-expanded multi-digraph and propose an efficient hybrid solution method that optimally solves real-world instances. To separate our work from recent research, we first briefly review related literature in Section 1.1 before further elaborating on our contributions in Section 1.2. We then outline the organization of our paper in Section 1.3.

### *1.1. Related Literature*

The DRSPMS combines aspects from crew scheduling, truck driver scheduling, and routing with synchronization, which we discuss in the following. In a broader sense, it also relates to routing with intermediate stops for purposes such as replenishment, refueling, or breaks, which has been vividly discussed in recent years. For an overview and classification of this research field, we refer to the comprehensive survey of Schiffer et al. (2019). Related problems in crew scheduling have been thoroughly studied in the past. A common assumption in crew scheduling is that trip or flight legs are fixed, such that the main optimization task is to assign crew members to these legs. This assumption does not hold for the DRSPMS, in which bus routes are not yet fixed. Instead, one or multiple intermediate stops at arbitrary service stations along or near the route may be inserted between any two regular bus stops. Furthermore, the DRSPMS does not require drivers to cover a leg or trip entirely, but allows them to only cover parts of it. Therefore, the DRSPMS includes additional routing decisions and synchronization requirements that are not present in crew scheduling problems. Due to these major differences, we do not study the literature on crew scheduling any further. Instead, we refer to Barnhart et al. (2003) and Deveci and Demirel (2018) for a survey on airline crew scheduling, to Heil et al. (2020) for railway crew scheduling, and to Ibarra-Rojas et al. (2015) for bus driver scheduling in public transport. The field of vehicle routing and truck driver scheduling combines scheduling breaks and rest periods for truck drivers with vehicle-related routing decisions but commonly considers vehicles and drivers as inseparable planning units. Contrarily, drivers can switch vehicles at arbitrary intermediate stops en route in the DRSPMS and must be treated as separate planning units while still synchronizing their routes. Due to the lack of synchronization requirements in vehicle routing and truck driver scheduling, we do not review work in this research field in more detail but refer to the survey of Koubâa et al. (2016) and, for more recent work on this topic, to Goel and Irnich (2016), Schiffer et al. (2017), and Tilk and Goel (2020). Table 1 compares major characteristics of the DRSPMS to related personnel scheduling problems, namely crew scheduling (CS) and vehicle routing and truck driver scheduling (VRTDS).

Table 1: Related crew and driver scheduling problems

	Assignment	Scheduling	Routing	Working hours	Intermediate stops	Synchronization
CS	✓	✓		✓		
VRTDS	✓	✓	✓	✓	✓	
DRSPMS	✓	✓	✓	✓	✓	✓

Due to the synchronization requirements, which result from the possibility of driver exchanges and dead-heading, the DRSPMS falls into the category of routing problems with synchronization constraints. This relatively new research field has gained increasing attention during the past two decades. For a comprehensive review and classification of synchronization in vehicle routing up to 2011, we refer to Drexel (2012). As pointed out by Drexel (2012), existing publications on vehicle routing with synchronization focus primarily on load synchronization (e.g., for transshipments) and on temporal synchronization of customer visits. Research addressing the temporal and spatial synchronization of non-autonomous vehicles to enable movements is still scarce. This so-called movement synchronization is relevant in various settings and applications, including N-echelon routing problems (see Guastaroba et al. 2016), active-passive vehicle routing problems (see Meisel and Kopfer 2014, Tilk et al. 2018), and the routing of workers and vehicles (see Kim et al. 2010, Fink et al. 2019). In the following, we survey only literature that considers movement synchronization in the context of vehicle and crew routing and scheduling as contained in the DRSPMS.

In simultaneous vehicle and crew routing and scheduling problems, vehicles and crews are non-autonomous objects who pair up to fulfill a given set of pickup and delivery requests. Furthermore, crews can usually change vehicles at a limited number of locations. Consequently, the routes of crews and vehicles must be synchronized. Hollis et al. (2006) study a simultaneous vehicle and crew routing and scheduling problem motivated by an application at Australia Post. In their problem setting, postal workers can switch vehicles only at depots and not during a trip. The authors present a set covering formulation and propose a column generation heuristic to solve the problem of finding minimum cost routes and schedules. They conduct a computational study with three real-world instances including up to 339 locations and 1,181 shipment requests and show that their heuristic terminates with an average optimality gap of 2.47% over all instances. Kergosien et al. (2011) address a joint vehicle and crew routing and scheduling problem arising in medical care. Ambulance drivers, physicians, and vehicles of different types must be routed at minimum costs to transport patients between various care units. Crews can change vehicles at depots only. The authors propose a tabu search algorithm to solve the problem and apply it to instances based on real-world data of a French hospital including 130 transportation requests per day on average. Simultaneous vehicle and crew routing and scheduling also arises in long-distance road transport. Drexel et al. (2013) consider a problem setting in which driver schedules are subject to the European working time regulations, and drivers can only change vehicles at a predefined set of relay stations after completing a daily rest. Furthermore, drivers can use shuttle services to travel between relay stations. Routes and schedules have to be determined for trucks and drivers to minimize fixed and variable costs. The authors develop a two-stage heuristic approach that first fixes truck movements and relay stations and subsequently decides on driver movements. Both stages are solved employing a large neighborhood search. A case study with real-world data of a major German freight forwarder comprising 2,800 shipment requests between 1,975 customer locations and 157 additional relay stations did not show notable cost savings resulting from the joint planning of vehicle and driver routes. However, the authors

state that this result might be due to the unsatisfactory performance of their algorithm and is valid only for their specific setup. Domínguez-Martín et al. (2018) study a simultaneous vehicle and crew routing and scheduling problem motivated by a real-world problem of local air traffic in the Canary Islands. Crews can switch aircraft at a limited number of airports, referred to as exchange locations. Aircraft and crew routes have to be determined such that distance-dependent costs are minimized. The authors formally define the problem through a mathematical model with additional valid inequalities and propose a branch-and-cut algorithm to solve the problem. They show in a numerical study on randomly generated test instances that their solution approach can solve instances with up to 30 nodes within a computation time of two hours. Lam et al. (2020) consider a similar problem inspired by an application in military air transportation. Crews can interchange vehicles at different customer locations and may travel as passengers before or after their duty. Lam et al. (2020) formulate an MIP model and a constraint programming model to find routes and schedules that minimize the number of vehicles and crews as well as the total distance traveled. They further present two matheuristics that combine both models with a large neighborhood search. Computational experiments on randomly generated instances, including up to 11 locations and 50 pickup-and-delivery pairs, show that the constraint-programming-based large neighborhood search outperforms MIP-based methods in terms of solution quality. The results also demonstrate that simultaneous routing of crews and vehicles yields notable benefits over sequential approaches. The possibility of vehicle interchanges is essential to obtain good solutions in this specific setting.

As can be seen, simultaneous vehicle and crew routing and scheduling problems arise in various applications. While all existing works consider crew members and vehicles as separate planning units and thus incorporate synchronization constraints, additional constraints vary with the underlying application. The possibility of driver exchanges is usually limited to small subsets of locations in order to reduce the problem complexity. Furthermore, many authors consider only simplified or problem-specific working time regulations, such as a maximum route duration. By contrast, the DRSPMS allows driver exchanges at all customer locations and arbitrary intermediate stops, and considers the official working time regulations imposed by the European Union. Note that the DRSPMS benefits from the fact that vehicle routes are partly fixed as the bus stops and their order are given. Therefore, the routing decisions for vehicles only concern the selection and placement of intermediate stops, which significantly reduces the problem complexity compared to common routing problems. At the same time, however, the large number of potential locations for driver exchanges increases the problem complexity considerably compared to classical crew scheduling problems. To summarize, the DRSPMS considered in this paper differs from existing literature in the field of simultaneous vehicle and crew routing and scheduling in several aspects. Table 2 compares the characteristics of the DRSPMS against the most closely related existing works. Despite its high relevance, no solution algorithm exists that captures all characteristics of the DRSPMS, namely i) driver exchanges at all customer locations, ii) driver exchanges at intermediate stops, iii) driver deadheading, and iv) European driving time regulations. Specifically, we are not aware of any publication considering driver exchanges at both regular and intermediate stops.

## 1.2. Contribution

In this paper, we close the research gap outlined in Section 1.1 by developing a scalable matheuristic that generates provably optimal solutions for a novel routing and scheduling problem motivated by an application in long-distance bus networks. Specifically, the contribution of our work is threefold:

Table 2: Key references on movement synchronization in vehicle and crew routing and scheduling

	Hollis et al. (2006)	Kergosien et al. (2011)	Drexl et al. (2013)	Dominguez- Martin et al. (2018)	Lam et al. (2020)	This paper
Driver exchanges at the depot	✓	✓				
Driver exchanges at customer locations				(✓)	✓	✓
Driver exchanges at intermediate locations			(✓)			✓
Driver deadheading				✓	✓	✓
EU driving time regulations			✓			✓

*Notes.* ✓: considered, (✓): partially considered

First, we introduce a new type of driver routing and scheduling problem with synchronization constraints. To the best of our knowledge, we are the first to consider driver routing and scheduling with synchronization constraints in the context of long-distance bus networks, where, contrary to other applications, drivers can change vehicles not only at customer stops but additionally at arbitrary intermediate stops en route. We develop a mathematical model of our problem based on a time-expanded multi-digraph and introduce valid inequalities to reduce the solution space. We further derive bounds for the total number of required drivers.

Second, we present a hybrid optimization algorithm that, motivated by the requirements of a real-world application, combines mathematical programming techniques with heuristic elements. Precisely, we alternate between a local search phase to generate solutions and an MIP implementation to prove optimality. This matheuristic enables us to provide feasible solutions within seconds even for large-scale instances while allowing for statements about the quality of obtained solutions. We further enrich this approach with a destructive bound improvement phase to tighten lower bounds and speed up convergence.

Third, we evaluate our solution approach in a comprehensive computational study with real-world data. The results show that our algorithm is readily applicable in practice. It provides feasible solutions for all instances and solves a huge variety of real-world instances to optimality in 205 seconds on average. Moreover, we derive insights for practitioners. Compared to current solutions deployed in practice, we can reduce the number of drivers required by up to 56%. We further show that the consideration of driver exchanges is beneficial in long-distance bus networks and leads to average savings of 43% per instance.

### 1.3. Organization

The remainder of this paper is structured as follows. First, we describe the problem setting for the DRSPMS in Section 2. In Section 3, we introduce a mathematical formulation of the problem and present our matheuristic. Section 4 specifies the experimental design for our real-world case study. We present computational results and provide managerial insights in Section 5. Finally, Section 6 concludes the paper by summarizing its main insights and suggesting directions for future research.

## 2. Problem Description

In the following, we introduce our planning problem. We first describe the practical application before specifying the driving and working time regulations that apply in long-distance bus networks in Europe. Finally, we formally define the DRSPMS.

### *2.1. Intercity Bus Driver Routing and Scheduling in Practice*

The deregulation of the European intercity bus market in the past decade has paved the way for new business models in this sector. Nowadays, many of the large coach companies in Europe are platform providers that outsource operational tasks to local bus companies, referred to as subcontractors in the following. These subcontractors provide buses and drivers and are responsible for executing trips. The platform provider maintains the digital marketplace and takes care of management duties, such as demand forecasting, network planning, bus assignments, or routing and scheduling of buses and drivers. In this paper, we consider the planning tasks of the platform provider, specifically the planning of driver routes and schedules.

Before creating driver schedules, the platform provider has to plan lines and rides. A line is a sequence of customer stops offered regularly. Once having defined a set of lines to be operated, the platform provider schedules the rides. A ride associates a line with a specific date and time. The platform provider does not fix ride departure times throughout the planning process but instead defines time windows based on target departure times resulting from expected customer demand. Here, we refer to a segment between two subsequent customer stops as a ride segment. Given a set of rides and the respective time windows, the platform provider defines driver routes and schedules such that every ride segment is covered by a driver. However, not necessarily the same driver has to cover the entire ride, but drivers may be swapped during the trip. Due to a persistent driver shortage, the platform provider is mainly interested in minimizing the total number of required drivers. Subcontractors often pursue additional objectives such as minimizing the overall workload to ensure driver happiness. Therefore, they might post-optimize driver routes constrained by the total driver count set by the platform provider. As this planning step is not within the scope of the platform provider, we do not consider it any further but refer to Online Appendix A for a description of how to integrate the subcontractors' objectives into the model developed in this paper.

In many countries, driver schedules are subject to strict driving time regulations that aim to protect driver working conditions and improve road safety. Such regulations limit, for example, the daily driving time or the maximum driving time without a break. However, in long-distance bus networks, many lines have a travel duration that exceeds these limits. For coach companies, having the driver take their break while passengers are waiting on the bus is unfavorable as it extends travel times and thus decreases customer satisfaction. Further, short travel times and direct connections with few stops are crucial to gain and sustain market share. Even for very long lines, including breaks can be disadvantageous as most customers travel only for a particular segment on the bus. Customers traveling a short ride segment (of, e.g., 2 hours) might not want their travel time to be interrupted by a break. Operating such lines permanently with two drivers could avoid breaks and extended travel times for passengers but would heavily increase operational costs.

As cost-efficient operations are essential for a coach company's success, coach companies prefer to exchange drivers instead of double-booking drivers on buses in order to reduce operational cost. Here, a sufficiently rested driver replaces an exhausted driver once she reaches her driving or working time limit. Contrary to other crew scheduling applications, these driver exchanges may not only take place at regular customer stops

but additionally at arbitrary service stations along or near the route. Here, driving a short detour to reach a service station is acceptable. Thus, both the drivers’ routes and the exact vehicle route for a ride must be defined. Specifically, the coach company has to assign drivers to bus rides and schedule the driver’s working, driving, and break times. For each ride, potential intermediate stops and exact departure times must be set. Note that we use the terms ride, vehicle route, and bus route interchangeably in the remainder of the paper. While drivers may use any means of transport to change their location, coach companies favor drivers to travel as passengers on their own bus lines to save costs. Therefore, we assume for the DRSPMS that drivers can only move by deadheading or steering a bus of their company.

## 2.2. Legal Framework in the European Union

We now specify the legal regulations that apply in our problem setting. For countries in the European Union, driving and working times of long-haul bus or truck drivers are regulated by the Regulation (EC) No 561/2006 (European Union 2006). Specifically, after a maximum steering period of 4.5 hours, drivers have to take a break of at least 45 minutes. This break can be split into two intervals of 15 minutes and 30 minutes. The total steering time per day is limited to 9 hours, whereas the daily working time must not exceed 13 hours. If at least two drivers are present for the entire time between two daily rest periods, the team’s working time can be increased up to 21 hours within a 30 hours period. Furthermore, drivers must not drive for more than 56 hours between two consecutive weekly rest periods and no more than 90 hours within two weeks. Additionally, numerous exceptions and application-specific rules apply.

As we aim to provide a proof of concept with this paper, we assume a planning horizon of a single day for the DRSPMS and therefore only consider rules applying to drivers’ daily working and steering times. Furthermore, we neglect the possibility of splitting breaks. However, integrating these rules into the basic model is a straightforward extension that we leave for future work. Table 3 gives an overview of the parameters relevant for the DRSPMS.

## 2.3. Problem Definition

After describing the practical motivation and the legal framework, we now formally define the DRSPMS and summarize all relevant notation in Table 4.

*Notation:* Consider a set of rides  $\mathcal{R}$  for a single day. Each ride  $r \in \mathcal{R}$  is associated with a pickup node  $p_r$  and a delivery node  $d_r$ , which represent the first and the last customer stop of a ride, respectively. Furthermore, we associate a ride  $r$  with a set of intermediate customer nodes  $\mathcal{I}_r$  that must be visited in a predefined order. This set is empty for rides consisting only of a single ride segment. In addition to the set of customer stops, defined as  $\mathcal{C}_r = \{p_r\} \cup \mathcal{I}_r \cup \{d_r\}$ , we consider a set of service stations  $\mathcal{S}_r$  for all rides  $r \in \mathcal{R}$  and a central depot  $v = 0$ , where a set of fully rested drivers  $\mathcal{K}$  is available. From this virtual depot, drivers can move instantaneously to any other location and back. Service stations can be used for

Table 3: Parameters imposed by the European Regulation (EC) No 561/2006

Parameter	Value	Description
$T^{cs}$	4.5 hours	Maximum steering time without taking a break
$T^{ds}$	9 hours	Maximum steering time per day (between two consecutive rest periods)
$T^{dw}$	13 hours	Maximum working time per day (between two consecutive rest periods)
$T^b$	45 minutes	Minimum break duration

intermediate stops, for example, to exchange drivers. Here, we consider only service stations that can be reached within a detour limit  $\zeta \ll T^b$ . We define node sets  $\mathcal{N}_r$  that include all nodes relevant for ride  $r \in \mathcal{R}$  (i.e.,  $\mathcal{N}_r = \mathcal{C}_r \cup \mathcal{S}_r$ ). Furthermore,  $\mathcal{N}$  denotes the set of relevant nodes over all rides, including the virtual depot (i.e.,  $\mathcal{N} = \cup_{r \in \mathcal{R}} \mathcal{N}_r \cup \{0\}$ ). We define time windows for all nodes  $v \in \mathcal{N} \setminus \{0\}$  as  $tw_v = [e_v, l_v]$ . These time windows implicitly define the precedence relations between customer nodes of the same ride and are of equal length  $\vartheta \ll T^b$ . Note that the time window size  $\vartheta$  must be greater than or equal to the detour limit  $\zeta$ . Otherwise, arrival times might be infeasible. To keep deviations from the minimum ride duration at a reasonable level, time window size  $\vartheta$  and detour limit  $\zeta$  have to take values significantly smaller than the minimum break duration  $T^b$ .

*Solution and Objective Function:* We aim to route and schedule drivers such that the total number of drivers is minimized while serving all ride requests and complying with relevant legal regulations. Specifically, a solution i) determines intermediate stops at service stations, ii) sets exact departure times at all nodes, iii) assigns drivers to ride segments, iv) specifies driver exchanges and deadheading, and v) sets breaks for all drivers.

*Constraints:* A solution to the DRSPMS is subject to the following constraints:

- Every ride  $r \in \mathcal{R}$  is covered by one or multiple drivers such that every customer node  $v \in \mathcal{C}_r$  is visited within its time windows  $tw_v$ .
- A driver can only cover a single ride at a time.
- Drivers can move only while being paired up with a vehicle and vice versa.
- Movements of drivers and vehicles are synchronized in time and space.
- Driver schedules comply with the legal regulations, specifically the limits  $T^{cs}$ ,  $T^{ds}$ , and  $T^{dw}$  are not exceeded and the minimum break duration  $T^b$  is fulfilled.
- Detours via service stations must not exceed the detour limit  $\zeta$ .

### 3. Methodology

In the following, we present a methodological framework to solve the DRSPMS. First, we introduce a graph representation in Section 3.1, which allows us to formulate a compact MIP in Section 3.2. We further enhance this MIP by adding valid inequalities and computing lower and upper bounds. We elaborate the bound computations in Section 3.3. Finally, we describe our matheuristic, which combines local search with mathematical programming techniques and a destructive bound improvement procedure in Section 3.4.

#### 3.1. Time-Expanded Directed Multi-Graph

In this section, we develop a graph representation that allows us to integrate some of the problem attributes, such as precedence constraints, the possibility of deadheading, or time windows, directly into the graph itself and thereby capture part of the problem complexity outside of the model.

We consider a time-expanded directed multi-graph  $\mathcal{G} = (\mathcal{V}, \mathcal{A})$  with a set of time-expanded nodes  $\mathcal{V}$  and a set of arcs  $\mathcal{A}$ . Every node  $i \in \mathcal{V}$  is associated with a non-time-expanded node  $v \in \mathcal{N}$  and a discrete time  $t_i$ . We derive relevant points in time based on the interval length  $\ell$ , which determines the granularity of time discretization in our graph and thus the approximation's accuracy to the time-continuous problem. While large intervals keep the number of time-discrete points low, thus reducing the problem complexity and model quality, shorter time intervals allow for a high-quality approximation but increase the computational

effort (cf. Boland et al. 2019). To overcome this trade-off, Boland et al. (2017) introduced the concept of dynamic discretization discovery for the continuous-time service network design problem. By iteratively discovering new points in time and adding them to a partially time-expanded network, the algorithm allows solving time-continuous problems to optimality by means of a time-discrete network (cf. Boland et al. 2017, Boland and Savelsbergh 2019). Applying dynamic discretization discovery to solve the DRSPMS is an interesting extension that we leave for future work.

For the DRSPMS, we choose the interval length  $\ell$  such that the time window size  $\vartheta$  is a multiple of it. We then create  $\frac{\vartheta}{\ell} + 1$  copies of every customer node  $v \in \cup_{r \in \mathcal{R}} \mathcal{C}_r$ . For service stations, we compute relevant times based on the preceding customer node and create a maximum of  $\frac{\vartheta}{\ell}$  copies per node. To obtain the subset of time-expanded nodes associated with a non-time-expanded node  $v \in \mathcal{N}$ , we define a mapping function  $\mathcal{T}(v) : \mathcal{N} \rightarrow \mathbb{P}(\mathcal{V})$ . Here,  $\mathbb{P}(\mathcal{V})$  denotes the power set of  $\mathcal{V}$ , including all subsets of  $\mathcal{V}$  with cardinality less than or equal to  $\frac{\vartheta}{\ell} + 1$ . To represent all feasible connections between time-expanded nodes  $i, j \in \mathcal{V}$ , we define the arc set  $\mathcal{A}$ , which includes depot arcs, steering arcs, deadheading arcs, and waiting arcs. Depot arcs include connections from and to the virtual depot 0 for every node  $i \in \mathcal{V} \setminus \{0\}$ , whereas steering arcs and deadheading arcs represent connections on which drivers might be steering or deadheading, respectively. Waiting arcs connect nodes associated with the same physical location. As there might be multiple arcs between any pair of nodes  $i, j \in \mathcal{V}$ , one for steering and one for deadheading, we introduce a set of modes  $m \in \mathcal{M}$  with  $\mathcal{M} = \{0, 1\}$  to differentiate arc types. We assign mode  $m = 1$  to all steering arcs and mode  $m = 0$  to all arcs on which drivers are not steering, that is, depot arcs, waiting arcs, and deadheading arcs. Thus, we characterize an arc by a triple  $(i, j, m)$  with origin  $i \in \mathcal{V}$ , destination  $j \in \mathcal{V}$ , and mode  $m \in \mathcal{M}$ . As described in Section 2.2, every driver has a certain amount of continuous steering time available, limited to  $T^{cs}$ . Steering reduces the remaining amount of this resource by the respective driving time. By taking a break of at least  $T^b$ , drivers can renew their steering time resource. Hence, we associate every arc  $(i, j, m) \in \mathcal{A}$  with a resource consumption  $c_{ijm}$ . For steering arcs, the resource consumption is equivalent to the corresponding driving time. For all other arcs, it is equal to zero or may even be negative for arcs which are sufficient to take a break and thus renew the steering time resource. We further use the set of arcs  $\mathcal{A}$  to implicitly model precedence constraints between customer nodes, the detour limit  $\zeta$ , and the maximum continuous steering time  $T^{cs}$ . Accordingly, an arc  $(i, j, m) \in \mathcal{A}$  only connects two vertices  $i, j \in \mathcal{V}$  if one of the following conditions holds: i) exactly one of the nodes represents the depot, ii) both nodes are customer nodes and node  $j$  is the immediate successor of  $i$ , iii) node  $j$  is a service station relevant for the segment between customer node  $i$  and its immediate successor, iv) node  $i$  is a service station relevant for the segment between customer node  $j$  and its immediate predecessor. Here, we consider only service stations that comply with the detour limit  $\zeta$ . Further, we include without loss of generality only arcs with a travel duration less than or equal to  $T^{cs}$  in our arc set  $\mathcal{A}$ .

We illustrate our graph representation in a simplified example. Consider customer nodes  $i$  and  $j$  associated with time windows  $tw_i$  and  $tw_j$ , respectively, and a ride segment from customer node  $i$  to customer node  $j$ . Additionally, there is a service station node  $s$ . As depicted in Figure 1, there are two possibilities to serve this ride segment, either driving directly from  $i$  to  $j$  or driving via service station  $s$ . Figure 2 shows the time-expanded multi-digraph for our example. For the sake of simplicity, we assume  $\ell = \vartheta$ , that is, we create only two copies of customer node  $i$ , for times  $t_i \in \{e_i, l_i\}$  such that  $\mathcal{T}(i) = \{i_1, i_2\}$ . The same holds for node  $j$ , respectively, such that  $\mathcal{T}(j) = \{j_1, j_2\}$ . As nodes  $i_1, i_2 \in \mathcal{V}$  refer to the same physical location, we

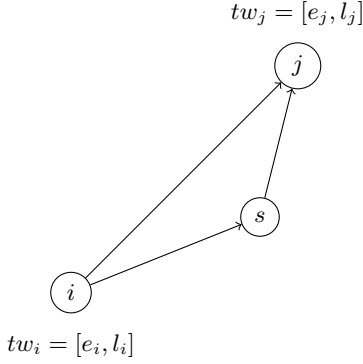


Figure 1: Ride example

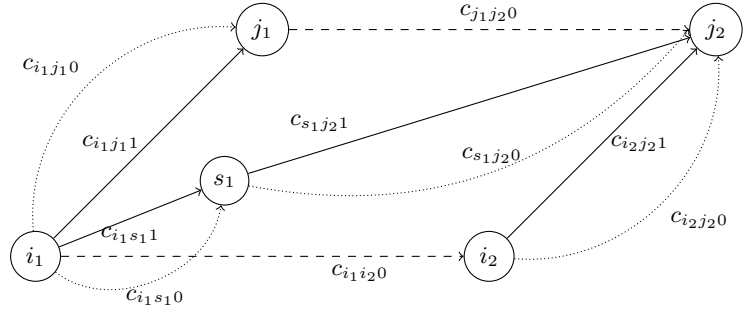


Figure 2: Graph representation

add a waiting arc from  $i_1$  to  $i_2$ . For the same reason, we add a waiting arc from  $j_1$  to  $j_2$ . To determine the time-copies of service station  $s$ , we consider its predecessor, customer node  $i$ . Given the set of relevant times for node  $i$ , we can compute the relevant times for  $s$  by simply adding the driving time from node  $i$  to node  $s$ . In general, driving via a service station leads to a detour. Therefore, we can never connect the first time-copy of a service station with the first time-copy of its succeeding customer node. Thus, the number of time-copies of a service station is strictly smaller than the number of time-copies needed for a customer node. Only a single copy of the service station is needed in this example. Departing from node  $i$  at the earliest time possible and driving via service station  $s$ , we cannot reach node  $j$  at time  $e_j$ . The next time copy that we can reach is node  $j_2$ . Thus, we connect node  $s_1$  with node  $j_2$ . When starting at node  $i_2$ , driving via a service station is not feasible as node  $j_2$  cannot be reached. Hence we do not create a second copy of node  $s$ . Note that we also connect node  $s_1$  with node  $j_2$  if the detour is smaller than the interval length  $\ell$ , i.e., we round up the actual arrival time to the next time-discrete value in our graph. Finally, we add all remaining feasible steering and deadheading arcs, represented by solid and dotted lines, respectively. For the sake of simplicity, we do not display depot arcs.

### 3.2. Mathematical Model

Using the graph representation developed in the previous section, we can now formulate a compact MIP model for the DRSPMS. We first introduce a basic formulation before we present additional inequalities to break symmetries and tighten the model.

We define the MIP on the time-expanded multi-digraph  $\mathcal{G} = (\mathcal{V}, \mathcal{A})$  described in Section 3.1. To denote out- and ingoing arcs from and into all nodes in a subset  $\mathcal{S} \subset \mathcal{V}$ , we define cut sets  $\delta^+(\mathcal{S}) = \{(i, j, m) \in \mathcal{A} : i \in \mathcal{S}, j \notin \mathcal{S}, m \in \mathcal{M}\}$  and  $\delta^-(\mathcal{S}) = \{(j, i, m) \in \mathcal{A} : i \in \mathcal{S}, j \notin \mathcal{S}, m \in \mathcal{M}\}$ , respectively. Furthermore, we define cut sets for out- and ingoing steering arcs as  $\delta_1^+(\mathcal{S}) = \{(i, j, m) \in \mathcal{A} : i \in \mathcal{S}, j \notin \mathcal{S}, m = 1\}$  and  $\delta_1^-(\mathcal{S}) = \{(j, i, m) \in \mathcal{A} : i \in \mathcal{S}, j \notin \mathcal{S}, m = 1\}$ . With a slight abuse of notation, we refer to cut sets of singletons  $\mathcal{S} = \{i\}$  by  $\delta(i)$  instead of  $\delta(\{i\})$ . We use binary variables  $x_{kijm}$  to state whether driver  $k \in \mathcal{K}$  traverses an arc  $(i, j, m) \in \mathcal{A}$  ( $x_{kijm} = 1$ ) or not ( $x_{kijm} = 0$ ) and derive exact bus routes from the driver routes in a postprocessing step. To track the drivers' steering resource levels, we introduce continuous variables  $r_{ki}$ , which determine the remaining amount of steering time driver  $k \in \mathcal{K}$  has at node  $i \in \mathcal{V}$ . With this notation as summarized in Table 4, a basic MIP for the DRSPMS holds as follows:

Table 4: Notation

Sets and Parameters	
$\mathcal{R}$	Set of rides
$\mathcal{K}$	Set of drivers
$\mathcal{I}_r$	Set of intermediate customer nodes of ride $r \in \mathcal{R}$
$\mathcal{C}_r$	Set of customer nodes of ride $r \in \mathcal{R}$ , $\mathcal{C}_r = \{p_r\} \cup \mathcal{I}_r \cup \{d_r\}$
$\mathcal{S}_r$	Set of service stations relevant for ride $r \in \mathcal{R}$
$\mathcal{N}_r$	Set of non-time-expanded nodes relevant for ride $r \in \mathcal{R}$ , $\mathcal{N}_r = \mathcal{S}_r \cup \mathcal{C}_r$
$\mathcal{V}$	Set of time-expanded nodes
$\mathcal{M}$	Set of modes $m \in \mathcal{M}$ , with $m = 1$ for steering arcs and $m = 0$ for all other arcs
$\mathcal{A}$	Set of feasible arcs $(i, j, m)$ between time-expanded nodes $i, j \in \mathcal{V}$ with mode $m \in \mathcal{M}$
$\mathcal{T}(v)$	Function mapping non-time-expanded node $v \in \mathcal{N}$ to the respective subset of time-expanded nodes, $\mathcal{T}(v) : \mathcal{N} \rightarrow \mathbb{P}(\mathcal{V})$
$\delta^+(\mathcal{S}), \delta^-(\mathcal{S})$	Cut sets of outgoing / ingoing arcs from / into subset $\mathcal{S} \subset \mathcal{V}$
$\delta_1^+(\mathcal{S}), \delta_1^-(\mathcal{S})$	Cut sets of outgoing / ingoing steering arcs from / into subset $\mathcal{S} \subset \mathcal{V}$
$p_r, d_r$	Pickup and delivery nodes of ride $r \in \mathcal{R}$
$c_{ijm}$	Resource consumption associated with arc $(i, j, m) \in \mathcal{A}$
$t_i$	Time associated with node $i \in \mathcal{V}$
Decision Variables	
$x_{kijm}$	Binary variables that indicate if driver $k \in \mathcal{K}$ traverses arc $(i, j, m) \in \mathcal{A}$ ( $x_{kijm} = 1$ ) or not ( $x_{kijm} = 0$ )
$r_{ki}$	Continuous variables that track the remaining amount of steering time for driver $k \in \mathcal{K}$ at node $i \in \mathcal{V}$

$$\min \quad z = \sum_{k \in \mathcal{K}} \sum_{(i,j,m) \in \delta^+(\mathcal{T}(0))} x_{kijm} \quad (1)$$

subject to

$$\sum_{(i,j,m) \in \delta^+(\mathcal{T}(0))} x_{kijm} \leq 1 \quad \forall k \in \mathcal{K} \quad (2)$$

$$\sum_{(j,i,m) \in \delta^-(i)} x_{kjim} = \sum_{(i,j,m) \in \delta^+(i)} x_{kijm} \quad \forall k \in \mathcal{K}, i \in \mathcal{V} \quad (3)$$

$$\sum_{i \in \mathcal{T}(v)} \sum_{k \in \mathcal{K}} \sum_{(i,j,m) \in \delta_1^+(i)} x_{kijm} = 1 \quad \forall r \in \mathcal{R}, v = p_r \quad (4)$$

$$\sum_{i \in \mathcal{T}(v)} \sum_{k \in \mathcal{K}} \sum_{(j,i,m) \in \delta_1^-(i)} x_{kjim} = 1 \quad \forall r \in \mathcal{R}, v = d_r \quad (5)$$

$$\sum_{k \in \mathcal{K}} \sum_{(i,j,m) \in \delta_1^+(i)} x_{kijm} = \sum_{k \in \mathcal{K}} \sum_{(j,i,m) \in \delta_1^-(i)} x_{kjim} \quad \forall r \in \mathcal{R}, v \in \mathcal{I}_r \cup \mathcal{S}_r, i \in \mathcal{T}(v) \quad (6)$$

$$x_{lij0} \leq \sum_{k \in \mathcal{K} \setminus \{l\}} x_{kijm} \quad \forall l \in \mathcal{K}, (i, j, m) \in \mathcal{A} : m = 1 \quad (7)$$

$$\sum_{\substack{(i,j,m) \in \mathcal{A}: \\ m=1}} c_{ijm} x_{kijm} \leq T^{ds} \quad \forall k \in \mathcal{K} \quad (8)$$

$$\sum_{i \in \mathcal{T}(0)} \sum_{(j,i,m) \in \delta^-(i)} t_j x_{kjim} - \sum_{i \in \mathcal{T}(0)} \sum_{(i,j,m) \in \delta^+(i)} t_j x_{kijm} \leq T^{dw} \quad \forall k \in \mathcal{K} \quad (9)$$

$$r_{kj} \leq r_{ki} - \sum_{\substack{m \in \mathcal{M}: \\ (i,j,m) \in \mathcal{A}}} (c_{ijm} x_{kijm}) + T^{cs} (1 - \sum_{\substack{m \in \mathcal{M}: \\ (i,j,m) \in \mathcal{A}}} x_{kijm}) \quad \forall k \in \mathcal{K}, (i,j) : (i,j,m) \in \mathcal{A} \quad (10)$$

$$x_{kijm} \in \{0, 1\} \quad \forall k \in \mathcal{K}, (i,j,m) \in \mathcal{A} \quad (11)$$

$$0 \leq r_{ki} \leq T^{cs} \quad \forall k \in \mathcal{K}, i \in \mathcal{V} \quad (12)$$

The objective function (1) minimizes the number of drivers leaving the depot, that is, the total number of drivers required. Constraint sets (2) - (6) regulate driver and requests flows in our network. Constraints (2) state that drivers can leave the depot only once and accordingly execute only a single route. Constraints (3) ensure flow consistency through the network for every driver. Constraint sets (4) - (6) require all requests to be served. While constraint sets (4) and (5) ensure that pickup and delivery nodes of every request  $r \in \mathcal{R}$  are visited, Constraints (6) guarantee the consistency of request flows at intermediate customer stops and at service station nodes. Constraints (7) allow deadheading for a driver  $l \in \mathcal{K}$  only if there is another driver  $k \in \mathcal{K} \setminus \{l\}$  steering on the same arc. To integrate working and driving time regulations, we further define Constraints (8) - (10). Constraints (8) and (9) limit the daily steering time and daily working time for each driver. Constraints (10) update the driver's steering resource level after traversing an arc. Finally, constraint sets (11) - (12) define the variables' domains.

To improve the MIP's performance, we formulate additional Constraints (13) - (16), which cut off symmetric solutions and tighten some variable assignments.

$$r_{ki} \geq T^{cs} \left( \sum_{(i,j,m) \in \delta^+(i)} x_{kijm} \right) \quad \forall k \in \mathcal{K}, i \in \mathcal{T}(0) \quad (13)$$

$$r_{ki} \leq T^{cs} \left( \sum_{(i,j,m) \in \delta^+(i)} x_{kijm} \right) \quad \forall k \in \mathcal{K}, i \in \mathcal{V} \quad (14)$$

$$\sum_{i \in \mathcal{T}(0)} \sum_{(i,j,m) \in \delta^+(i)} x_{kijm} \geq \sum_{i \in \mathcal{T}(0)} \sum_{(i,j,m) \in \delta^+(i)} x_{lijm} \quad \forall k \in \{1, \dots, |\mathcal{K}| - 1\}, l = k + 1 \quad (15)$$

$$\sum_{i \in \mathcal{T}(0)} \sum_{(i,j,m) \in \delta^+(i)} t_i x_{kijm} \geq \sum_{i \in \mathcal{T}(0)} \sum_{(i,j,m) \in \delta^+(i)} t_i x_{lijm} \quad \forall k \in \{1, \dots, |\mathcal{K}| - 1\}, l = k + 1 \quad (16)$$

Constraints (13) initialize the resource level of activated drivers, whereas Constraints (14) fix the resource level  $r_{ki}$  to zero if driver  $k \in \mathcal{K}$  never visits node  $i \in \mathcal{V}$ . Next, Constraints (15) and (16) break some of the symmetry in the solution space by activating drivers one after another and assigning routes to drivers by descending departure times.

### 3.3. Bound Computations

To iterate over drivers in our mathematical model, we calculate an artificial upper bound for the number of drivers. We compute a simple upper bound by considering the drivers' scarcest resource, the continuous steering time  $T^{cs}$ , assuming that there is no possibility of renewing this resource, that is, we neglect any possibility of taking a break. We thus divide every ride  $r \in \mathcal{R}$  into  $s_r$  segments of total driving times less than or equal to  $T^{cs}$  and assume that a new driver is assigned to each segment. Then, the total number of segments over all rides gives an upper bound for the number of required drivers, see Equation (17). We use

the resulting upper bound  $UB$  to define the cardinality of the set of drivers  $\mathcal{K} = \{1, \dots, UB\}$ .

$$UB = \sum_{r \in \mathcal{R}} s_r \quad (17)$$

Preliminary computations showed the linear programming (LP) relaxation of the MIP defined in Section 3.2 to be rather weak. Therefore, we derive two constructive lower bounds that further strengthen the MIP formulation. For a computational analysis of the different lower bounds, we refer to Online Appendix B. We compute a first constructive lower bound by relaxing some of the legal regulations, particularly the limit on the continuous steering time  $T^{cs}$ . We divide the minimum total steering time by the maximum daily steering time per driver ( $T^{ds}$ ). Here, the minimum total steering time is the sum of driving times over all direct steering arcs between customer locations, such that our first lower bound  $LB_1$  results in:

$$LB_1 = \lceil \left( \sum_{(i,j,m) \in \mathcal{A}: i,j \in \cup_{r \in \mathcal{R}} \mathcal{C}_r, m=1} c_{ijm} \right) / T^{ds} \rceil \quad (18)$$

This approach assumes a perfect spatial and temporal fit between all rides, allowing drivers to utilize their available daily steering time perfectly. It also assumes that drivers can always drive directly from one customer stop to the next without a detour via any service station. Further, it disregards any conflicts between rides. Therefore, it constitutes a rather weak lower bound, particularly for instances involving many short rides taking place simultaneously as these cannot be executed by the same driver. Therefore, we derive a second lower bound  $LB_2$  by determining the number of parallel rides  $r_t$  per time interval  $t \in \mathcal{T}$ . Here, we first obtain time intervals  $t \in \mathcal{T}$ , representing minimum overlaps resulting from the latest start and earliest arrival times at regular customer stops of all rides. For every time interval  $t \in \mathcal{T}$ , we then count the number of rides active within this interval. The maximum ride count defines the minimum number of drivers required simultaneously:

$$LB_2 = \max_{t \in \mathcal{T}} (r_t) \quad (19)$$

As neither of the two approaches is provably superior over the other, we always compute both lower bounds and take the maximum value as a global lower bound  $LB$ :

$$LB = \max(LB_1, LB_2) \quad (20)$$

Given lower bound  $LB$ , we can further improve our MIP by adding constraints (21) - (23). Note that lower bounds  $LB_1$ ,  $LB_2$ , and  $LB$  are independent of the level of time discretization and are also valid for the original (time-continuous) problem as described in Section 2.

$$\sum_{k \in \mathcal{K}} \sum_{i \in \mathcal{T}(0)} \sum_{(i,j,m) \in \delta^+(i)} x_{kijm} \geq LB \quad (21)$$

$$\sum_{i \in \mathcal{T}(0)} \sum_{(i,j,m) \in \delta^+(i)} x_{kijm} \geq 1 \quad \forall k \in \{1, \dots, LB\} \quad (22)$$

$$\sum_{i \in \mathcal{T}(0)} \sum_{(j,i,m) \in \delta^-(i)} x_{kjim} \geq 1 \quad \forall k \in \{1, \dots, LB\} \quad (23)$$

Constraint (21) sets the lower bound for the total number of required drivers. Given this lower bound and our symmetry breaking Constraints (15) - (16), we force drivers with an index up to the lower bound to be activated, that is, they must have an active arc to and from the depot, as stated in Constraints (22) - (23).

### 3.4. Destructive-Bound-Enhanced Matheuristic

Due to the inherent complexity of the DRSPMS, the basic MIP implementation is not tractable for real-world instances. Preliminary experiments showed that commercial MIP solvers are able to solve small instances but fail to find feasible solutions for real-world-sized instances even after hours of computations. Accordingly, motivated by our real-world application, we aim at developing a solution approach that is readily applicable in practice. This approach must provide feasible high-quality solutions within a reasonable amount of computational time. In fact, as saving a single driver may lead to significant cost reductions, we aim to find optimal solutions. While branch-and-price approaches are state-of-the-art for routing problems, the presence of synchronization requirements causes considerable difficulties with labeling algorithms commonly used in branch-and-price to solve the pricing problem (cf. Drexel 2012). Alternative branch-and-price methods that are tailored to solving such a pricing problem solve only relatively small instances to optimality (cf. Tilk et al. 2019). Synchronization constraints also lead to difficulties with classical improvement heuristics that assume independence of routes (cf. Drexel 2012). Thus, it remains an open question which methods are most effective for solving routing problems with synchronization constraints. Accordingly, a large variety of different solution methods often tailored to the specific problem at hand exists. To satisfy the requirements from the real-world application of the DRSPMS, we propose a matheuristic that provides feasible solutions quickly through its heuristic components while still converging to provably optimal solutions. To speed up convergence, we further enrich our matheuristic with a destructive improvement phase. Following recent performance improvements of mathematical programming solvers, matheuristics have become increasingly popular for various problems and application areas. For other works that apply similar concepts, we refer the interested reader to, e.g., Larrain et al. (2017), Lam et al. (2020), and Yin et al. (2021).

Algorithm 1 outlines the general structure of our DBMH. First, we use a construction heuristic to generate a feasible start solution. We further improve this solution by applying a local search procedure. If the objective value of the resulting solution  $S$  equals the constructive lower bound  $LB$ , solution  $S$  is optimal, and

---

**Algorithm 1:** Destructive-bound-enhanced matheuristic

---

**Input:** Constructive lower bound  $LB$ , time limits  $\eta, \eta^{LB}, \eta^{MIP}, \eta^{LS}$

- 1  $S \leftarrow \text{ConstructionHeuristic}()$
- 2  $S \leftarrow \text{LocalSearch}(S, \eta)$
- 3 **if**  $f(S) = LB$  **then**
- 4      $\underline{\text{return } S}$
- 5  $LB, S \leftarrow \text{DestructiveBoundImprovement}(LB, S, \eta^{LB})$
- 6 **if**  $f(S) = LB$  **then**
- 7      $\underline{\text{return } S}$
- 8 **while**  $\eta$  not reached **do**
- 9      $S, LB \leftarrow \text{SolveMIP}(LB, S, \eta^{MIP})$
- 10     $S \leftarrow \text{LocalSearch}(S, \eta^{LS})$
- 11 **return**  $\underline{S}$

---

we terminate the search. Otherwise, we invoke a destructive bound improvement procedure to improve the lower bound for our problem. If the initial solution  $S$  is proven to be optimal during this phase or an optimal solution  $S^*$  is found, we stop. Otherwise, we enter the hybrid optimization phase, which is inspired by the variable MIP neighborhood descent of Larrain et al. (2017). This approach enriches the implementation of an MIP by a heuristic component. Specifically, the underlying idea is to alternate between a local search phase to generate improved solutions and the MIP to prove optimality. Here, we start from an initial solution  $S$  and a destructive lower bound  $LB$ , and solve the MIP defined in Sections 3.2 and 3.3 until one of the following three conditions holds: i) optimality is proven, ii) we find a new incumbent, or iii) we reach a time limit. Note that we first run the MIP without providing a start solution and inject the initial solution  $S$  only if the MIP solver did not obtain any feasible solution after the time limit  $\eta^{MIP}$ . In case of proven optimality or timeout, the algorithm terminates. By optimality we mean optimality of the time-discrete problem, which is not necessarily optimal for the original (time-continuous) problem. Solutions, for which optimality is proven by means of the constructive lower bounds, however, are truly optimal, both for the time-discrete and the time-continuous problem. If we find a new incumbent, we reinvoke the local search based on the new solution  $S$  and continue iterating between the local search phase and the MIP phase. Note that the MIP phase might also update the current lower bound  $LB$ . Contrary to Larrain et al. (2017), who explore neighborhoods by solving constrained subproblems with an MIP solver, we implement all heuristic components outside of the MIP implementation. This has proven to be computationally more efficient for the DRSPMS as MIP solvers still suffer from slow convergence for constrained variants of the original problem and show difficulties finding new feasible solutions quickly. Furthermore, we follow a best-improvement strategy whereas Larrain et al. (2017) switch back to the full MIP with the first improvement found.

In the remaining sections, we describe the components of our matheuristic in more detail. First, we outline the destructive bound improvement in Section 3.4.1. Next, we explain the solution representation used in the heuristic components in Section 3.4.2 before we describe the construction heuristic in Section 3.4.3. Finally, we specify the local search phase in Section 3.4.4. We provide a computational analysis on the impact of all components on the solution quality in Online Appendix C.

### 3.4.1. Destructive Bound Improvement

Preliminary computations in the development phase showed that the hybrid optimization approach enriching the MIP implementation by a local search component as in Larrain et al. (2017) had difficulties raising the lower bound and therefore converged rather slowly for many instances. To tighten our lower bounds and accelerate convergence, we introduce a destructive bound improvement phase based on the idea presented in Klein and Scholl (1999) for solving the resource-constrained project scheduling problem. Klein and Scholl (1999) differentiate two main classes for computing lower bounds for minimization problems. Constructive bounds are computed using direct methods, such as solving the LP relaxation. Destructive bounds, on the other hand, are computed by imposing a bound on the objective function and then trying to contradict the feasibility of this restricted problem. When setting the upper bound to a low value, the search space of feasible solutions is reduced significantly and might even be empty. Klein and Scholl (1999) propose working with the LP relaxation of the original problem when applying destructive techniques. Due to the weak LP relaxation of our problem, however, we work with the restricted integer problem instead.

Algorithm 2 outlines the main steps of this procedure. Given an initial constructive lower bound  $LB$  for our original problem  $P$ , we first check whether we can prove the initial solution  $S$  to be optimal. If

---

**Algorithm 2:** Destructive bound improvement

---

**Input:** Constructive lower bound  $LB$ , initial solution  $S$ , time limit  $\eta^{LB}$

```
1 while  $\eta^{LB}$  not reached do
2   if  $f(S) = LB$  then
3     return  $\underline{S}$ 
4   Build  $P(LB) : \sum_{k \in \mathcal{K}} \sum_{(i,j,m) \in \delta^+(\mathcal{T}(0))} x_{kijm} \leq LB$ 
5   Solve  $P(LB)$ 
6   if feasible solution  $S$  then
7     return  $\underline{S}$ 
8   if  $P(LB)$  is infeasible then
9      $LB \leftarrow LB + 1$ 
10 return  $\underline{LB}$ 
```

---

this is not the case, that is,  $f(S) > LB$ , we create a restricted problem  $P(LB)$  by adding the constraint  $\sum_{k \in \mathcal{K}} \sum_{(i,j,m) \in \delta^+(\mathcal{T}(0))} x_{kijm} \leq LB$ . We then try to solve this restricted problem  $P(LB)$  using a standard solver. If a feasible solution  $S$  is found, we terminate and return  $S$  as this is an optimal solution for our original problem  $P$ . If the restricted problem is proven infeasible, we increment our lower bound  $LB \leftarrow LB + 1$  and restart the improvement phase. We repeat these steps until we prove optimality or reach a time limit. If we reach the time limit  $\eta^{LB}$  without a feasible solution, the current lower bound  $LB$  is a valid lower bound for our original problem  $P$ . Note that, in contrast to the constructive lower bounds defined in Section 3.3, the destructive lower bound depends on the level of time discretization and thus only holds for the time-discrete problem as defined in Section 3.2.

### 3.4.2. Solution Representation and Evaluation

For the heuristic components of our solution approach, we choose a solution representation that considers only a subset of the decision variables defined in Section 3.2. Specifically, we present a solution as a collection of driver routes. Thus, we model only arcs that are traversed in the current solution (i.e.,  $(i, j, m) \in \mathcal{A} : \sum_{k \in \mathcal{K}} x_{kijm} \geq 1$ ). Furthermore, we consider only drivers that execute at least one segment of a ride and refer to this subset of active drivers in a solution  $S$  as  $\bar{\mathcal{K}}(S) \subseteq \mathcal{K} : \sum_{(i,j,m) \in \mathcal{A}:m=1} x_{kijm} \geq 1 \forall k \in \bar{\mathcal{K}}$ . We assign every driver  $k \in \bar{\mathcal{K}}$  a route  $\varrho_k$  through our time-expanded multi-digraph  $\mathcal{G}$ . A route consists of an ordered list of arcs  $(i, j, m)$  to be traversed by the respective driver, such that  $x_{kijm} = 1 \forall (i, j, m) \in \varrho_k$ . Departure times  $t(S)$  can be derived from the times  $t_i$  associated with the nodes  $i \in \mathcal{V}$  that are included in the driver routes of solution  $S$ . Note that we do not explicitly model the resource variables  $r_{ki}$  but instead check a solution for resource feasibility after every modification of the driver routes. Then, we can derive the objective function value  $f(S)$  associated with a solution  $S$  from the cardinality of the subset  $\bar{\mathcal{K}}(S)$ , such that  $f(S) = |\bar{\mathcal{K}}|$ . Considering only arcs with mode  $m = 1$ , we can derive the exact routes for each bus ride, which we also refer to as vehicle routes  $\Upsilon(S)$ .

### 3.4.3. Construction Heuristic

To construct an initial solution, we use a greedy two-step approach that first fixes vehicle routes and schedules and, second, defines driver routes and schedules. As the number of drivers is not limited, we can always generate a feasible solution. To create vehicle routes, we assume that all ride segments are served

without intermediate stops at service stations. We further fix the departure times of all ride segments to the earliest time possible. Based on the resulting vehicle routes, we assign drivers as follows. For every vehicle route, starting from the one with the earliest start time, we apply the following steps:

1. If a driver is available at the start node and can execute the first segment, we assign her to the current vehicle route. Otherwise, we add a new driver. We let the selected driver steer until i) the vehicle route is completed or ii) the driver reaches her continuous steering time limit  $T^{cs}$ .
2. In case of i), we let the current driver and all deadheading drivers wait at the terminal node until they can take over another vehicle route or have exhausted their total working time.
3. In case of ii), we decide whether to let the driver wait at the current stop or whether to stay on the bus (deadheading). If another bus later visits this stop and the waiting time is sufficient to take a break of  $T^b$  but no longer than a predefined upper bound, e.g.,  $4T^b$ , the driver waits. Otherwise, the driver deadheads.

We continue Steps 1 - 3 until we assigned all ride segments. The resulting vehicle routes  $\Upsilon(S)$ , departure times  $t(S)$ , and driver routes  $\varrho(S)$  define our start solution  $S$ .

#### 3.4.4. Local Search in a Composite Neighborhood

In contrast to Larrain et al. (2017), who complement their MIP with a variable neighborhood descent, we apply a local search based on a composite neighborhood, which has proven to be more efficient for the DRSPMS. We apply this local search procedure to improve solutions provided by the construction heuristic and by the MIP solver. Composite neighborhoods have already been used successfully by other authors (see, e.g., Schiffer and Walther 2018, Schneider and Löffler 2019). For computational analysis of the different neighborhood search variants, we refer to Online Appendix D.

We define our composite neighborhood through  $\kappa$  operators. In every iteration of our local search, we select the best solution  $S$  in our composite neighborhood. We continue this search until we reach a time limit or no further improvement is possible, indicating that we found a local optimum with respect to our composite neighborhood, and return the best solution found so far.

All  $\kappa$  operators in our composite neighborhood follow a best-improvement strategy, that is, they modify the current solution until no further improvement is possible. In every iteration, multiple new solutions are generated. Any of these new solutions can then be further explored and serves as a basis for creating multiple modified solutions in the next iteration. However, exploring all these possible modifications would result in an unreasonable computational effort. Moreover, many of the solutions show only minor structural differences but have the same objective function value because small changes, such as shifting the departure time of a single ride segment, do not necessarily affect the total number of drivers needed. Therefore, we focus only on a small subset of promising solutions. We introduce a secondary objective as a tiebreaker that allows us to differentiate and rank solutions with the same primary objective value. This secondary objective accounts for the remaining amount of working time  $\theta(S)$  of drivers who are active in the current solution  $S$ , considering only the remaining working time before starting or after finishing their route:

$$\theta(S) = \sum_{k \in \mathcal{K}} \left( T^{dw} - \left( \sum_{(j,i,m) \in \delta^-(\mathcal{T}(0))} t_i x_{kjim} - \sum_{(i,j,m) \in \delta^+(\mathcal{T}(0))} t_i x_{kijm} \right) \right) \quad (24)$$

Solutions with a high remaining working time  $\theta(S)$  might offer a higher potential for consolidating driver routes and thus allow for reducing the number of drivers. Hence, we order solutions with identical primary objective function values by decreasing amount of remaining working time and consider only the first  $\mu(\%)$  out of this list in each iteration. At minimum, we keep an absolute number of  $\mu^{min}$  solutions per iteration.

Due to the synchronization requirements present in the DRSPMS, standard local search operators are not applicable. Instead, we developed seven problem-specific operators. These operators address different problem attributes, precisely the composition of driver routes  $\varrho(S)$ , the composition of vehicle routes  $\Upsilon(S)$ , and the departure times  $t(S)$  in a solution  $S$ . Table 5 provides an overview of these operators, which are defined as follows:

*Reassign Segments.* This operator assumes fixed vehicle routes  $\Upsilon(S)$  and departure times  $t(S)$  for all ride segments and tries to reassign ride segments to drivers. For every driver route in the current solution, we check whether we can assign the ride segments to other drivers. A driver  $k$  can be discarded if all ride segments in her route  $\varrho_k(S)$  can be added to existing routes of the other drivers  $l \in \bar{K}(S) : l \neq k$ . This operator aims at improving the solution by eliminating drivers, which directly impacts the objective value.

*Postpone.* This operator aims to delay some of the departure times  $t(S)$  of the current solution  $S$ , which might allow for more efficient driver schedules. Accordingly, this operator utilizes the time windows of our problem. After shifting the departure times of one or multiple rides, we recompute the driver routes  $\varrho(S)$ , while vehicle routes  $\Upsilon(S)$  remain unchanged. To update the driver routes, all operators use the procedure described in Section 3.4.3.

*Prepone.* Similar to the *Postpone* operator, the *Prepone* operator aims at improving the current solution  $S$  by shifting some of the departure times  $t(S)$  and obtaining better driver routes  $\varrho(S)$ . While the *Postpone* operator delays the departure times of selected rides, the *Prepone* operator shifts the departure of selected rides to earlier points in time. Again, vehicle routes  $\Upsilon(S)$  remain unchanged.

*Insert Intermediate Stop (Random).* The previously presented operators focus on adjusting driver routes and departure times while fixing the vehicle routes. In contrast, the operator *Insert Intermediate Stop (Random)* modifies the vehicle routes  $\Upsilon(S)$  by inserting intermediate stops at service stations for potential driver

Table 5: Local search operators

Operator	Modifies	Size
Reassign Segments	$\varrho(S)$	$\mu \sum_{n=1}^{ \mathcal{RS} -1} \frac{ \mathcal{RS} !}{( \mathcal{RS} -n)!}$
Postpone	$t(S), \varrho(S)$	$\mu 2^{\frac{\vartheta}{\ell}}  \mathcal{R} $
Prepone	$t(S), \varrho(S)$	$\mu 2^{\frac{\vartheta}{\ell}}  \mathcal{R} $
Insert Intermediate Stop (Random)	$\Upsilon(S), t(S), \varrho(S)$	$\mu 2^{\frac{\vartheta}{\ell}}  \mathcal{R} $
Insert Intermediate Stop (Shortest Detour)	$\Upsilon(S), t(S), \varrho(S)$	$\mu 2^{\frac{\vartheta}{\ell}}  \mathcal{R} $
Insert Intermediate Stop (Synchronization Potential)	$\Upsilon(S), t(S), \varrho(S)$	$\mu 2^{\frac{\vartheta}{\ell}}  \mathcal{R} $
Remove Intermediate Stop	$\Upsilon(S), t(S), \varrho(S)$	$\mu 2^{\frac{\vartheta}{\ell}}  \mathcal{R} $

Notes.  $\mathcal{RS}$ : Set of ride segments.

exchanges. First, we choose a ride segment to insert an intermediate stop. Here, we prioritize segments with long durations as splitting these into shorter segments might allow for more flexible and thus more efficient driver routing. However, for the sake of diversification, we do not strictly select the ride segment with the longest travel duration but rather randomize the selection to a certain degree controlled by a perturbation factor  $p$ . Given a list of  $n$  ride segments ordered by their descending travel duration, we draw a random number  $y \in [0, 1)$  and select the ride segment at position  $\lfloor y^n n \rfloor$ . Second, we randomly choose a service station reachable within the detour limit to insert into this ride segment, which changes some of the departure times  $t(S)$ . We adjust the vehicle route accordingly. Finally, we update the driver routes  $\varrho(S)$ .

*Insert Intermediate Stop (Shortest Detour).* The operator *Insert Intermediate Stop (Shortest Detour)* modifies vehicle routes by inserting intermediate stops at service stations. However, instead of selecting a service station randomly, we now choose a service station based on the additional driving time that the change implies. As in the previously described operator, we first select a ride segment. Here, we prioritize ride segments with long travel times. Next, we rank all service stations according to the descending detour they cause. From this list we do not simply select the station leading to the shortest detour but again randomize the selection as we do for the selection of ride segments. Then, we adjust the vehicle routes  $\Upsilon(S)$  and departure times  $t(S)$  accordingly and finally update the driver routes  $\varrho(S)$ .

*Insert Intermediate Stop (Highest Synchronization Potential).* As the two preceding operators, this operator modifies vehicle routes by inserting intermediate stops at service stations. Here, we select service stations based on their synchronization potential, which we define through the number of nodes in routes of the current solution that share the same physical location. Given a list of service stations ordered by their descending synchronization potential, we again randomize the selection of service stations. Based on the selected service station, we adjust the vehicle routes  $\Upsilon(S)$  and departure times  $t(S)$  and update the driver routes  $\varrho(S)$ .

*Remove Intermediate Stop.* This operator aims at removing redundant stops at service stations to create more efficient driver routes and schedules. It modifies the vehicle routes  $\Upsilon(S)$  in a solution  $S$  by eliminating intermediate stops until no further improvement is possible. Then, we recompute departure times  $t(S)$  and driver routes  $\varrho(S)$  accordingly.

## 4. Experimental Setup

This section defines the experimental design for our computational study. In Section 4.1, we describe our real-world instances before we specify the experimental setting for our computational study in Section 4.2.

### 4.1. Instances

We derive our instances from a large real-world data set provided by Flixbus, a leading coach company in Europe. This data set comprises more than 3,000 rides to be executed all over Europe on a single day in the summer high season of 2019. It includes all stops to be visited on each ride, scheduled departure times at bus stops, the travel duration for every ride segment, and the subcontractor responsible for executing the ride. Additionally, Flixbus provided us with the geocoordinates of service stations available for driver exchanges. To approximate the travel duration to and from service stations, we first calculate the orthodromic distance with the Haversine formula and then multiply this distance with a conversion factor provided by Flixbus.

We create instances from this data set as follows: first, we transform the scheduled departure time  $\tau_v$  of every customer node  $v \in \mathcal{N} \setminus \{0\}$  into time windows  $[e_v, l_v]$  of width  $\vartheta$ , such that  $e_v = \tau_v - \frac{\vartheta}{2}$  and  $l_v = \tau_v + \frac{\vartheta}{2}$ . Based on the time window of a node and the level of time discretization  $\ell$ , we define the set of discrete departure times as described in Section 3.1. Next, we exclude service stations that cannot be visited within the detour limit  $\zeta$  for each ride. Finally, as drivers may steer only buses of their company, we separate the data by subcontractor, which leads to 351 instances. These instances vary considerably in terms of size and complexity. Therefore, we cluster them into three groups depending on the number of time-expanded arcs  $\mathcal{A}$ : i) small instances with  $|\mathcal{A}| < 1,000$ , ii) medium instances with  $1,000 \leq |\mathcal{A}| < 5,000$ , and iii) large instances with  $5,000 \leq |\mathcal{A}|$ . Table 6 gives an overview of aggregated instance attributes for each group, displaying the number of rides ( $|\mathcal{R}|$ ), the number of ride segments ( $|\mathcal{RS}|$ ), the number of non-time-expanded nodes ( $|\mathcal{N}|$ ), the number of customer locations ( $\sum_{r \in \mathcal{R}} |\mathcal{C}_r|$ ), and the number of available service stations ( $\sum_{r \in \mathcal{R}} |\mathcal{S}_r|$ ). For all instances, we consider a time window width of  $\vartheta = 10$  minutes, a detour limit of  $\zeta = 10$  minutes, and a time discretization of  $\ell = 10$  minutes, if not stated otherwise. Note that we further decompose some of the instances into independent sub-instances. If a subcontractor operates multiple ride sets that do not share any bus stops or service stations, there is no possibility to transfer drivers between rides of different sets. Consequently, we optimize driver routes and schedules for these sets independently.

#### 4.2. Algorithm Design and Parameter Fitting

We executed all numerical experiments in a single core setting on a cluster of 812 machines, each having 28 Intel Xeon E5-2690 v3 processors (2.6 GHz) with 32 GB RAM each, running on Linux. Both the MIP and our matheuristic were implemented as a single core thread using the Gurobi Python Interface with Gurobi 9.1.1 and Python 3.8.8. In our matheuristic, we use Gurobi callbacks to alternate between the MIP and the local search phase. We set the time limit to 3,600 seconds for all methods.

We fitted the algorithmic parameters of our matheuristic based on a subset of 35 instances, including 10% of all instances per instance size. Initial value sets for the algorithmic parameters have been identified during preliminary computations in the development phase. In a systematic study, we tested these predefined sets by varying a single parameter at a time and fixing it to the value providing the best results. Table 7 gives an overview of the parameter values considered and highlights final values in bold for the time limit

Table 6: Aggregated instance attributes

Instance size	# Instances		$ \mathcal{R} $	$ \mathcal{RS} $	$ \mathcal{N} $	$\sum_{r \in \mathcal{R}}  \mathcal{C}_r $	$\sum_{r \in \mathcal{R}}  \mathcal{S}_r $
Small	101	Average	2	13	73	15	58
		Median	2	12	67	14	50
		Minimum	1	4	13	5	2
		Maximum	6	34	155	38	136
Medium	158	Average	6	34	274	40	233
		Median	6	32	257	37	216
		Minimum	2	11	55	14	10
		Maximum	22	85	621	96	556
Large	92	Average	24	154	3,543	178	3,368
		Median	17	111	1,044	127	867
		Minimum	4	22	320	26	238
		Maximum	168	1,153	74,130	1,321	74,013

Table 7: Parameter setting

Parameter	$\eta^{LB}$			$\eta^{LS}$			$\mu$		
Values	5%	10%	<b>15%</b>	5%	<b>10%</b>	15%	<b>1%</b>	10%	20%
$\Delta z$ [%]	0.48	0.32	0.06	0.45	0.06	0.17	0.06	0.28	0.44
Parameter	$\eta^{MIP}$			$p$			$\mu^{min}$		
Values	20%	<b>50%</b>	80%	3	<b>5</b>	10	<b>10</b>	15	20
$\Delta z$ [%]	0.28	0.06	0.46	0.46	0.06	0.46	0.06	0.28	0.44

of the destructive bound improvement phase ( $\eta^{LB}$ ), the time limit of the MIP solver before injecting a start solution ( $\eta^{MIP}$ ), the time limit of the local search phase during callbacks ( $\eta^{LS}$ ), the perturbation factor ( $p$ ), the share of solutions kept ( $\mu$ ), and the absolute minimum number of solutions kept ( $\mu^{min}$ ). The table further displays the average deviation over 10 runs from the best solution found with respect to the objective function value ( $\Delta z$ ). Note that the best parameter setting results in an average deviation of 0.06%, indicating that no global best setting for all instances exists.

Next, we use the same subset of instances for our algorithm design. In particular, we are interested in the performance gain resulting from enhancing a basic matheuristic, such as a warm-started MIP, with a local search (LS) component providing an improved start and the destructive bound improvement phase (DBI) component lifting the lower bound. Therefore, we compute 10 runs for every instance and compare the results of three different matheuristic variants: i) the MIP warm-started with the construction heuristic (CH) solution (CH+MIP), ii) the MIP warm-started with the CH+LS solution (CH+LS+MIP), and iii) the full destructive-bound-enhanced matheuristic (DBMH) as described in Section 3.4. Over all instances, warm-starting the MIP with the CH+LS start solution reduces the number of drivers by up to 7 compared to the CH solution and increases the number of instances solved to optimality within the time limit by 6.54%. Moreover, the computational time for instances solved to optimality can be reduced by 23.63% or 51.33 seconds on average. The results further show that the lower bound increases much faster when integrating the DBI, leading to better convergence and reducing computational times for instances solved to optimality by 54.87% or 169.44 seconds on average. We illustrate the impact of the LS and the DBI components in Figure 3, which plots the development of lower and upper bounds for three exemplary instances of small and medium size. The plots for instance III show that an improved start solution is particularly effective with a tight lower bound. While it takes the CH+LS+MIP method more than 3,000 seconds to lift the lower bound and prove optimality of the CH+LS start solution, the DBMH needs less than 400 seconds to terminate. Furthermore, the DBI cannot only prove optimality of heuristic start solutions but also finds optimal solutions while checking for feasibility of a particular objective function value, as the plots for instance II demonstrate. Here, the DBI starts from a constructive lower bound  $cLB = 4$  and finds a feasible and hence optimal solution with an objective function value of 4 while checking for feasibility of  $LB = UB = 4$ . Over all test runs, the DBMH solves 5.26% more instances to optimality than the CH+LS+MIP method. As expected, tight lower and upper bounds improve convergence, significantly reducing computational times for instances solved to optimality by 70.14%. Therefore, we chose the DBMH with advanced start and destructive bound improvement over the basic warm-started MIP variants.

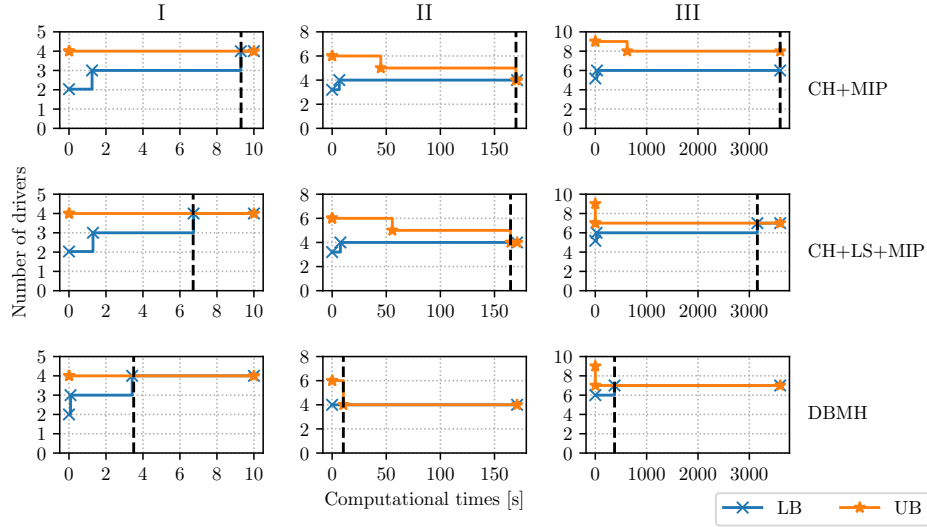


Figure 3: Convergence of CH+MIP, CH+LS+MIP, and DBMH

## 5. Results

This section presents the results of our computational study. We first evaluate the performance of our approach in Section 5.1. In Section 5.2, we analyze the performance of the individual algorithmic components. Finally, we derive managerial insights in Section 5.3.

### 5.1. Computational Performance

To validate the performance of our DBMH, we compare its results to solutions of the MIP and to heuristic solutions, considering all 351 real-world instances. We generate heuristic solutions by applying the CH first and the LS afterward. We conducted 10 runs per instance for every solution approach. Table 8 provides an overview of the aggregated results by instance size and solution method. The table header states the number of instances (# Instances) and the average best driver count per instance (Average best  $z$ ) for each instance size. In the table's main body, we report the percentage of instances solved to optimality (opt.solved[%]), the average computational time to optimality (t[s]), the average gap between the best solution and the best bound (gap[%]), the average deviation from the best-known solution ( $\Delta z$ [%]), and the accumulated driver count over all instances per instance size ( $\sum z$ ) for every solution method. The results in Table 8 demonstrate that our DBMH outperforms the MIP and the CH+LS on real-world instances. Specifically, on medium and large instances, our matheuristic solves more instances to proven optimality than the MIP. This result demonstrates the relevance of the heuristic components and the destructive bound improvement for obtaining optimal solutions. Moreover, these additional components allow us to reduce computational times by 79.42% for small instances compared to the MIP. Another advantage of our approach is its ability to provide feasible solutions for all instances within seconds. By contrast, the MIP fails to find any feasible solution for the majority of medium and large instances, which is why we cannot state the MIP's average gap, deviation from best-known solutions, and total driver count for these instances. While the combination of CH and LS performs best with respect to computational times, its solutions deviate by 10.39% on average from best-known solutions and require a total of 155 additional drivers compared to the DBMH, indicating

Table 8: Aggregated results on real-world instances

Instance size		Small	Medium	Large	All
# Instances		101	158	92	351
Average best $z$		2.63	6.58	29.75	11.52
MIP	opt.solved[%]	99.55	51.25	1.60	53.02
	t[s]	26.43	312.98	1,849.17	162.34
	gap[%]	0.00	-	-	-
	$\Delta z$ [%]	0.00	-	-	-
	$\sum z$	266	-	-	-
DBMH	opt.solved[%]	100.00	60.00	4.26	57.69
	t[s]	5.44	422.13	709.00	204.53
	gap[%]	0.00	6.81	32.12	11.77
	$\Delta z$ [%]	0.00	0.24	0.06	0.12
	$\sum z$	266	1,042	2,739	4,047
CH+LS	opt.solved[%]	68.70	24.43	2.15	32.09
	t[s]	0.02	0.45	97.57	24.39
	gap[%]	8.33	17.45	33.58	19.23
	$\Delta z$ [%]	11.61	15.10	1.60	10.39
	$\sum z$	300	1,157	2,745	4,202

the importance of the destructive bound improvement and the MIP to reach optimal solutions. For large instances, however, the deviation of heuristic solutions from best-known solutions is relatively low with 1.60% as our matheuristic often terminates without finding the optimal solution in these cases.

Recalling the requirements resulting from the practical application described at the beginning of Section 3.4, the results in Table 8 indicate that our DBMH is the most appropriate solution method for practical applications as it generates feasible solutions quickly and provides information about the obtained solution quality.

## 5.2. Performance of the Algorithmic Components

We now analyze the impact of the components of our DBMH on solution quality and computational time in detail.

*Impact of Destructive Bound Improvement.* First, we study the impact of the DBI on the lower bound considering all 351 real-world instances. Table 9 depicts the average (avg) and median (med) improvement of the destructive lower bound (dLB) compared to the constructive lower bound (cLB),  $\Delta LB = \frac{dLB - cLB}{cLB}$  [%], grouped by instance size. Figures 4 and 5 contain additional information on the distribution of the bound improvement. By definition,  $dLB \geq cLB$  holds. As can be seen, the DBI increases the lower bound significantly and by 20.14% on average. The dLB is particularly effective for small and medium instances. The large delta between average and median improvement as well as the boxplots in Figures 4 and 5 show that the level of improvement varies notably depending on the instance size. While the DBI achieves significant bound improvements of up to 100% or three drivers for some instances, there exist many small and large instances for which the DBI cannot improve the cLB. Recalling the results from Table 8, there are two reasons for this observation: first, trivial instances can already be solved optimally through the CH, the LS, and the cLB, and hence no further bound improvement is possible. Second, large instances may bear a complexity for which the DBI is not able to improve the bound in the given time limit.

Table 9: Impact of destructive bound improvement

Instance size	$\Delta LB[\%]$	
	avg	med
Small	26.55	0.00
Medium	17.58	16.67
Large	2.99	0.00
All	20.14	0.13

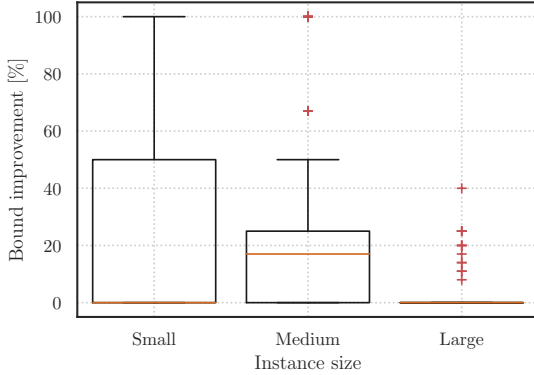


Figure 4: Relative bound improvement

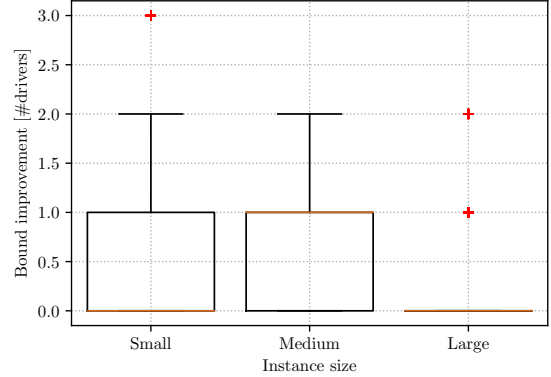


Figure 5: Absolute bound improvement

*Quality of Bounds and Start Solutions.* Next, we analyze the tightness of both lower bounds as well as the quality of the constructive and the improved start solution. In this context, we analyze the average deviation over 10 runs from the optimal solution ( $\Delta z[\%]$ ) for the cLB, the dLB, the initial solution obtained by the CH, and the improved initial solution after applying the LS. Table 10 depicts aggregated results grouped by instance size, while Figure 6 shows boxplots of the deviation for every instance size. Note that for this and the remaining analyses in this section, we only use instances solved to optimality, which include 101 small, 95 medium, and 3 large instances. Figure 6 shows that the quality of the lower bounds and the start solutions varies notably among different instances, in particular for small instances. While the cLB, the dLB, the CH, and the LS match the optimal objective function value for more than half of the small instances, there exist some instances for which the cLB deviates up to -50% and the start solutions deviate up to 100% from the optimal objective function value. Only the dLB is generally tight, deviating by -1.65% on average from the optimal solution as the results in Table 10 and Figure 6 show. In absolute terms, the cLB and dLB deviate from the optimal driver count by up to -3 and -2 drivers, respectively. The heuristic start solutions are far from optimal solutions, with a  $\Delta z$  per instance of up to 6 drivers for the CH and up to 4 drivers for the LS, which is in line with the results in Table 8. Overall, the average quality of the bounds and the start solutions decreases with growing instance size.

*Generation and Proof of Optimal Solutions.* Next, we investigate which algorithmic components generate and prove optimal solutions. We differentiate four stages in which optimality can be found: i) after generating an initial solution by applying the CH and the LSInit, ii) after applying the LS in the callback procedure (CB), iii) during the DBI, or iv) while solving the MIP. Table 11 shows the percentage share of instances solved to

Table 10: Average quality of bounds and start solutions

Instance size	$\Delta z$ [%]			
	cLB	dLB	LS	CH
Small	-15.70	0.00	11.97	15.27
Medium	-18.93	-3.47	18.59	24.40
Large	-17.78	-5.56	31.11	31.11
All	-17.23	-1.65	15.15	19.62

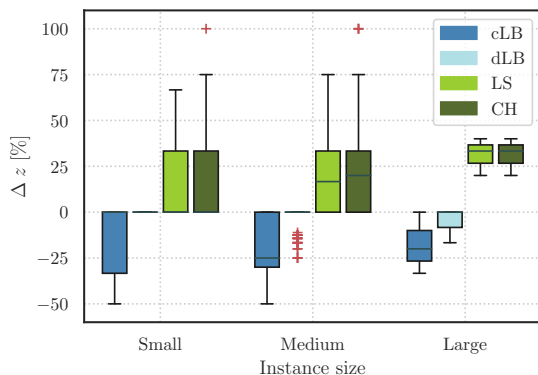


Figure 6: Deviation from optimal objective value

optimality in each stage. The results in Table 11 demonstrate why our matheuristic outperforms the MIP and combination of CH and LS. While the heuristic components can find optimal solutions in particular for small instances, MIP components, primarily the DBI, are essential to find and prove optimal solutions for larger instances. Specifically, the heuristic start solution is optimal for 54.88% of all instances, which explains the low computational times of our solution approach for small instances. Although the heuristic components cannot provide optimal solutions for large instances, they are still important for providing feasible solutions. For the majority of instances not solved to optimality within the time limit, the heuristic start solution cannot be improved any further by the MIP. This explains the rather low deviation of the CH+LS solutions from best-known solutions for large-size instances in Table 8.

*Distribution of Computational Time.* Finally, we analyze the distribution of computational time among the different algorithmic components. Due to large differences in absolute computational times, we show the percentage of the total computational time for every component and instance. Table 12 shows the aggregated computational time shares grouped by component and the average computational time per instance in seconds (t[s]) per instance size. As the results in Table 12 show, the MIP components account for 66.79% of the total computational time on average. For small instances, the computational times are evenly distributed between creating the start solution and the DBI. With growing instance size, the percentage share of computational time spent in heuristic components decreases due to two reasons: first, the growth rate of total computational times of the heuristic components is lower than the growth rate of MIP components. Second, as reported in Table 11, heuristic components are less successful in providing optimal or near-optimal solutions for large instances, and hence more time is spent in the MIP components. Also for instances not solved to optimality, solving the MIP accounts for the major part of the computational time. In contrast, the time for the DBI converges to its time limit  $\eta^{LB}$ . Computational times of the heuristic components add up to less than 1% on average for instances not solved to optimality.

To conclude, the combination of heuristic elements with mathematical programming techniques enriched by a destructive bound improvement procedure enables our matheuristic to quickly solve real-world instances to optimality and to provide feasible solutions even for large instances within seconds.

Table 11: Components finding optimal solutions

Instance size	Heuristic components		MIP components	
	Init	CB	DBI	MIP
Small	68.40%	-	31.60%	-
Medium	40.16%	0.84%	46.58%	12.42%
Large	-	-	66.67%	33.33%
All	54.88%	0.39%	38.77%	5.96%

Table 12: Computational time distribution

Instance size	t[s]	Heuristic components		MIP components	
		Init	CB	DBI	MIP
Small	7.20	48.55%	0.00%	51.45%	0.00%
Medium	448.68	16.31%	0.01%	70.46%	13.22%
Large	669.23	0.27%	0.15%	80.22%	19.36%
All	217.38	33.20%	0.01%	60.50%	6.29%

### 5.3. Managerial Insights

To derive managerial insights, we first compare our results to solutions currently obtained in practice and investigate the advantages of jointly considering all lines of one subcontractor compared to an isolated planning per line. Second, we evaluate the benefit of driver exchanges and intermediate stops. Finally, we study the impact of time windows, detour limits, and time discretization on solution quality and computational effort.

*Status Quo Comparison.* In practice, driver assignments are planned manually by a team of network planners, each being responsible for a set of lines. Due to the size and complexity of instances on subcontractor level and the lack of sufficient software tools, drivers are scheduled for every line separately. This means that the network planner applies a similar logic as used in the construction heuristic described in Section 3.4.3. Therefore, we divide all 351 instances into subinstances at the line level and apply the construction heuristic to approximate manual solutions. To compare our methodology against this status quo benchmark, we apply our DBMH first to line-based instances and second to subcontractor-based instances. We then compare both results to the approximated manual results. Table 13 shows the average (avg) and median (med) savings per instance as well as the total driver count reduction ( $\Delta \sum z$ ) for both comparisons grouped by instance size and instance type. The results in Table 13 show that our matheuristic outperforms the status quo benchmark. Over all line-based instances, we can improve manual solutions by 11.18% per instance on average, obtaining larger savings of 22.62% with growing instance size. When considering subcontractor-based instances, we can further increase the average savings to 13.07%. This result indicates that the primary savings result from the algorithm itself and only a minor part results from existing synergies between lines of the same subcontractor. Note that, in particular for small and medium instances, most instances do not have relevant synchronization potentials between lines, see Figure 7. Only a small number of instances shows synergies between lines and hence considerable savings of up to 50%, adding up to a reduction of 19 drivers over all instances.

Table 13: Savings compared to the status quo used in practice

Instance size	Line			Subcontractor		
	avg	med	$\Delta \sum z$	avg	med	$\Delta \sum z$
Small	8.87%	0.00%	35	10.28%	0.00%	41
Medium	13.50%	12.50%	73	15.85%	16.67%	85
Large	22.62%	25.00%	5	27.38%	28.57%	6
All	11.18%	0.00%	113	13.07%	5.56%	132

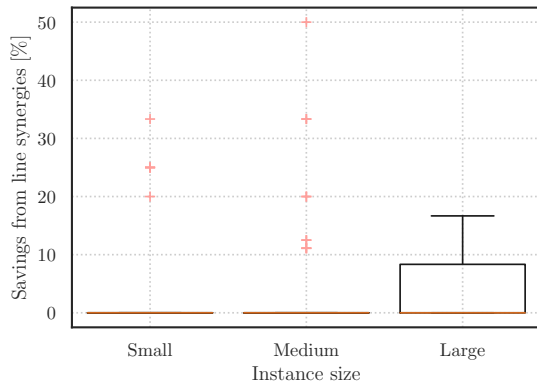


Figure 7: Savings from synergies between lines

In summary, our DBMH is able to improve the results currently achieved in practice. To reach globally optimal solutions, coach companies should optimize driver routes and schedules on subcontractor level. However, considering subcontractor-based instances is beneficial only for some instances and increases the problem complexity significantly.

*Benefit of Driver Exchanges and Intermediate Stops.* A unique characteristic of the DRSPMS is the consideration of intermediate stops for driver exchanges. On ride segments with a duration of more than  $T^{cs}$  hours, a stop at a service station is required to make this segment feasible. However, on all other ride segments, stops at service stations are optional but may enable more efficient operations. While a large number of service stations for driver exchanges might increase the potential for cost savings, it also increases the problem complexity. In this context, we analyze the savings potential from driver exchanges in general and from considering driver exchanges at intermediate stops in addition to driver exchanges at regular stops. Here, we consider only instances solved to optimality. To get a sufficiently large set of optimally solved instances for these analyses, we increase the time limit for medium and large instances to 2 and 4 hours, respectively. Furthermore, we study the impact of intermediate stops on computational efficiency.

First, we compare solutions with driver exchanges at intermediate stops to solutions without driver exchanges. Here, we consider the possibility of double driver teams for rides with a duration exceeding the continuous steering time limit  $T^{cs}$ . It is worth mentioning that without the possibility of driver exchanges, 176 of the 351 instances are infeasible as they include rides with a travel duration higher than the daily driving time of a double-driver team. Table 14 shows the average and median savings per instance as well as the total driver count reduction ( $\Delta \sum z$ ) from considering driver exchanges grouped by instance size. Note

that we only take instances into account that were solved optimally in both settings, such that our comparison bases on 149 instances in total, including 82 small, 60 medium, and 7 large instances. The results reported in Table 14 demonstrate the importance of driver exchanges for obtaining cost-efficient driver routes and schedules. Introducing the possibility of driver exchanges at regular and intermediate stops improves the solution quality by 42.69% on average compared to solutions without driver exchanges. Over all 149 instances, the consideration of driver exchanges reduces the total number of required drivers by 406. Note that also for instances not solved to optimality within the time limit, the solutions with driver exchanges consistently improve solutions without driver exchanges.

Next, we evaluate the savings potential from considering driver exchanges at intermediate stops in addition to driver exchanges at regular stops. Therefore, we compare optimal driver counts for the problem with DE-RIS (DE-RIS) to optimal driver counts for the problem with DE-RS (DE-RS). To compute solutions for the problem without intermediate stops, we set the detour limit  $\zeta$  to zero and apply our DBMH. Note that 14 out of 351 instances are infeasible in the DE-RS setting due to ride segments exceeding the continuous steering time limit  $T^{cs}$ . Only when allowing driver exchanges at intermediate stops all 351 instances are feasible. Table 15 shows the average and median savings per instance as well as the total driver count reduction ( $\Delta \sum z$ ) grouped by instance size. Our comparison includes all 220 instances solved to optimality in both settings, that is 100 small, 112 medium, and 8 large instances. For 19 instances (5 small, 13 medium, 1 large), the consideration of intermediate stops results in improved solutions and reduces the total driver count by 20 drivers or 17.54%. Figure 8 plots the distribution of savings for these instances. For the remaining instances, the driver count difference is zero, which explains the comparatively low average savings per instance of 1.64% reported in Table 15. Over all 220 instances solved to optimality, the option of driver exchanges at intermediate stops reduces the total driver count from 897 to 877 drivers, corresponding to a

Table 14: Savings from driver exchanges

Instance size	Average	Median	$\Delta \sum z$
Small	39.87%	50.00%	124
Medium	46.88%	50.00%	244
Large	39.73%	50.00%	38
All	42.69%	50.00%	406

Table 15: Savings from intermediate stops

Instance size	DE-RIS vs. DE-RS		
	Average	Median	$\Delta \sum z$
Small	1.13%	0.00%	5
Medium	2.13%	0.00%	14
Large	1.11%	0.00%	1
All	1.64%	0.00%	20

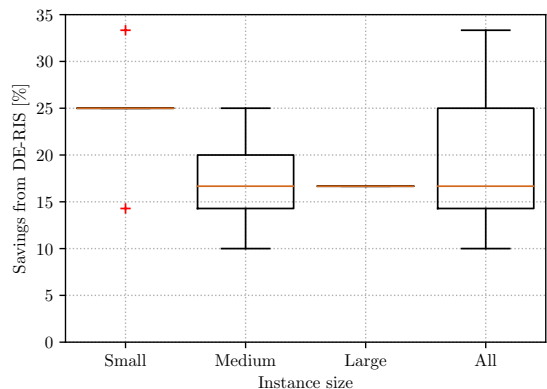


Figure 8: Distribution of savings from intermediate stops

decrease of 2.23%.

Finally, we analyze the impact of intermediate stops on problem complexity and computational efficiency. Here, we consider all 337 instances feasible with and without intermediate stops. The consideration of intermediate stops offers additional flexibility and the potential to reduce the number of drivers required but also substantially increases the problem complexity and, thus, the computational effort. Specifically, computational times to optimality are 745.67 seconds higher on average than when considering driver exchanges only at regular bus stops. Furthermore, without intermediate stops, 55 more instances can be solved to proven optimality within the given time limit. Moreover, as the problem with intermediate stops is harder to solve, we might obtain worse solutions for some instances within the given time limit than we do for the problem without intermediate stops within the same time limit. This is the case for 9.20% of the instances. Recall, however, that solutions for the problem without intermediate stops are also feasible for the problem with intermediate stops, which implies that we can always use the solution without intermediate stops for the problem with intermediate stops if the former is better. Nevertheless, developing a method that can effectively and consistently exploit the potential of intermediate stops for large instances is an important step for future research. In this regard, adapting existing column generation approaches for integrated crew scheduling problems with retiming options, such as the methodology proposed by Kliewer et al. (2012) or Bach et al. (2016) to include intermediate stops, seems promising.

In conclusion, driver exchanges at regular customer stops are essential to obtain feasible and cost-efficient driver routes and schedules. For some instances, the additional consideration of intermediate stops leads to further cost savings. Moreover, intermediate stops are required to ensure feasibility in some cases.

*Impact of Different Detour Limits and Time Windows.* In general, the number of intermediate stops considered and thus the computational effort depend on two main factors: the detour limit  $\zeta$  and the departure time window size  $\vartheta$ , which are closely related as described in Section 2.3. Consequently, we jointly examine the effect of different detour limits and time window sizes. Table 16 shows the average deviation from best-known solutions for different detour limits ( $\zeta[\text{min}]$ ) and time window sizes ( $\vartheta[\text{min}]$ ). To evaluate the impact on the solution quality, we only consider 135 instances solved to optimality in all settings. Furthermore, we do not differentiate by instance size as the size depends on the number of arcs, which differ with time window width and detour limit. The results in Table 16 demonstrate that the configuration providing the largest degree of freedom (i.e.,  $\vartheta = 30$  minutes and  $\zeta = 30$  minutes) yields the best results. This degree of freedom reduces the total driver count by 6 compared to a rather restricted setting with  $\vartheta = 10$  minutes and  $\zeta = 5$  minutes. Note that the impact of the time window size  $\vartheta$  is higher than the impact of the detour limit  $\zeta$ . Specifically, if the time window is sufficiently large, the detour limit can be set to a small value without any loss in solution quality. A higher detour limit can only achieve better results for narrow time windows. However, higher detour limits and wider time windows come at the expense of higher computational times. Increasing the time window size  $\vartheta$  from 10 minutes to 30 minutes increases the computational effort by more than a factor 100 on average. The impact of the detour limit on computational times is lower. A change of the detour limit  $\zeta$  from 5 minutes to 30 minutes yields a computational time increase of less than factor 10. Consequently, a setting that balances solution quality and computational times (e.g.,  $\vartheta = 10$  minutes and  $\zeta = 5$  minutes) should be chosen for practical applications. Note that large time windows are generally unfavorable in practice because, in addition to driver routing and scheduling, many other planning problems, e.g., bus assignments, depend on the target departure times.

*Impact of Different Time Discretization Levels.* Finally, we examine the impact of time discretization on solution quality and computational effort. The granularity of the time discretization in our underlying network determines the solution quality. Increasing the level of detail and thus the degree of freedom in departure times increases the computational effort but might allow for more efficient driver routes. To study this effect, we compute results for all 351 instances considering a time interval length of  $\ell = 5$  minutes and compare them to our results considering a time interval length of  $\ell = 10$  minutes. Table 17 gives an overview of the share of instances solved to optimality (opt.solved[%]), the average deviation from best-known solutions for instances solved optimally in the respective setting ( $\Delta z^*$ [%]), the average deviation from best-known solutions for all instances ( $\Delta z$ [%]), and the average computational time ( $t$ [s]) per instance. As can be seen, the increased problem complexity outweighs the potential for better solution quality. While this increased level of detail leads to improved optimal solutions for three instances with a reduction of one driver each, the solution quality for instances not solved to optimality is worse with a time discretization of  $\ell = 5$  so that the total driver count increases by 45. Furthermore, the computational time to optimality is higher by a factor of 11 on the same instances, and the share of instances solved to optimality within the time limit decreases by 11.84%. Consequently, for practical applications that aim for a fair balance between solution quality and computational effort, we consider a time discretization of  $\ell = 10$  minutes to be sufficient.

## 6. Conclusion and Outlook

In this paper, we presented a new type of driver routing and scheduling problem motivated by a practical application in long-distance bus networks. A unique characteristic of this problem is the possibility of driver exchanges at intermediate stops, which requires spatial and temporal synchronization of driver routes. We presented a mathematical formulation defined on a time-expanded multi-digraph. Furthermore, we proposed a solution approach that extends an MIP implementation by heuristic components and a destructive bound improvement procedure. We used real-world data provided by one of Europe’s leading coach companies to validate our DBMH. Our solution approach solves instances with up to 390 locations and 70 ride segments to optimality with an average computational time under 210 seconds. Even for large-scale instances we can provide feasible solutions within seconds. In contrast, standalone MIP solvers fail to find feasible solutions for a third of the instances even after one hour. Compared to standalone MIP solvers, our matheuristic improves computational times by 79.42% for small instances. Moreover, compared to current solutions deployed in practice, we can reduce the number of drivers required by 13.07% on average. Routing and scheduling drivers at the subcontractor level allows utilizing synergies between lines, leading to more efficient solutions. We further demonstrated that the consideration of driver exchanges is beneficial in long-distance bus networks

Table 16: Impact of different detour limits and time windows

		$\vartheta$ [min]			Avg
		10	20	30	
$\zeta$ [min]	5	1.60%	0.25%	0.00%	0.62%
	10	1.50%	0.25%	0.00%	0.60%
	20	-	0.25%	0.00%	0.12%
	30	-	-	0.00%	0.00%
Avg		1.55%	0.25 %	0.00%	-

Table 17: Impact of time discretization

	$\ell$ [min]	
	5	10
opt.solved [%]	50.86	<b>57.69</b>
$\Delta z^*$ [%]	<b>0.00</b>	0.48
$\Delta z$ [%]	2.11	<b>0.32</b>
t[s]	199.13	<b>18.53</b>

and leads to average savings of 42.69%. Considering driver exchanges at intermediate stops in addition to driver exchanges at regular stops allows for further cost savings, in particular for small and medium instances. For large instances, such a comparison cannot be drawn as many instances cannot be solved to optimality.

Our results show that the instances differ significantly in terms of synchronization potential, which raises a variety of interesting research questions. For example, using machine learning approaches to identify attributes that indicate which instances have a high chance of benefiting from the consideration of driver exchanges at intermediate stops or planning on subcontractor level might be a worthwhile research direction. Next, exploiting decomposition-based matheuristics that leverage column generation for subproblems also arising in railway or airline crew scheduling, i.e., problems in which trip legs and departure times are fixed, remains an interesting avenue for future research. Furthermore, adapting existing column generation approaches to consider intermediate stops seems promising. Another path for future research is to integrate the DRSPMS with other so far separately solved planning problems such as the assignment of rides to buses. From a methodological and a practical point of view, including uncertainty of travel times and developing a robust solution approach is another important step. Finally, studying the potential of driver exchanges en route in other real-world applications such as truck platooning, particularly with increasing automation levels, seems promising.

## **Acknowledgments**

We thank Dr. Berit Johannes and colleagues from Flix SE for providing and assisting with the real-world data set, and for providing valuable input and feedback. The authors gratefully acknowledge the computational and data resources provided by the Leibniz Supercomputing Centre ([www.lrz.de](http://www.lrz.de)).

## **Funding**

This work is funded by the Deutsche Forschungsgemeinschaft (DFG, German Research Foundation) – Project Number 277991500.

## **Declaration of Interest**

None.

## References

- Bach, Lukas, Twan Dollevoet, Dennis Huisman. 2016. Integrating Timetabling and Crew Scheduling at a Freight Railway Operator. *Transportation Science* **50**(3) 878–891.
- Barnhart, C., A. M. Cohn, E. L. Johnson, D. Klabjan, G. L. Nemhauser, P. H. Vance. 2003. Airline Crew Scheduling. R. W. Hall, ed., *Handbook of Transportation Science*. International Series in Operations Research & Management Science, Springer US, Boston, MA, 517–560.
- Boland, N., M. Hewitt, L. Marshall, M. Savelsbergh. 2017. The Continuous-Time Service Network Design Problem. *Operations Research* **65**(5) 1303–1321.
- Boland, N., M. Hewitt, L. Marshall, M. Savelsbergh. 2019. The price of discretizing time: A study in service network design. *EURO Journal on Transportation and Logistics* **8**(2) 195–216.
- Boland, Natashia L., Martin W. P. Savelsbergh. 2019. Perspectives on integer programming for time-dependent models. *TOP* **27**(2) 147–173.
- Deveci, M., N. Ç. Demirel. 2018. A survey of the literature on airline crew scheduling. *Engineering Applications of Artificial Intelligence* **74** 54–69.
- Domínguez-Martín, B., I. Rodríguez-Martín, J.-J. Salazar-González. 2018. The driver and vehicle routing problem. *Computers & Operations Research* **92** 56–64.
- Drexl, M. 2012. Synchronization in Vehicle Routing—A Survey of VRPs with Multiple Synchronization Constraints. *Transportation Science* **46**(3) 297–316.
- Drexl, M., J. Rieck, T. Sigl, B. Press. 2013. Simultaneous Vehicle and Crew Routing and Scheduling for Partial- and Full-Load Long-Distance Road Transport. *Business Research* **6**(2) 242–264.
- European Union. 2006. Regulation (EC) No 561/2006 of the European Parliament and of the Council of 15 March 2006 on the harmonisation of certain social legislation relating to road transport. *Official Journal of the European Union* **102** 1–13.
- Fink, M., G. Desaulniers, M. Frey, F. Kiermaier, R. Kolisch, F. Soumis. 2019. Column generation for vehicle routing problems with multiple synchronization constraints. *European Journal of Operational Research* **272**(2) 699–711.
- Goel, A., S. Irnich. 2016. An Exact Method for Vehicle Routing and Truck Driver Scheduling Problems. *Transportation Science* **51**(2) 737–754.
- Guastaroba, G., M. G. Speranza, D. Vigo. 2016. Intermediate Facilities in Freight Transportation Planning: A Survey. *Transportation Science* **50**(3) 763–789.
- Heil, J., K. Hoffmann, U. Buscher. 2020. Railway crew scheduling: Models, methods and applications. *European Journal of Operational Research* **283**(2) 405–425.
- Hollis, B. L., M. A. Forbes, B. E. Douglas. 2006. Vehicle routing and crew scheduling for metropolitan mail distribution at Australia Post. *European Journal of Operational Research* **173**(1) 133–150.
- Ibarra-Rojas, O. J., F. Delgado, R. Giesen, J. C. Muñoz. 2015. Planning, operation, and control of bus transport systems: A literature review. *Transportation Research Part B: Methodological* **77** 38–75.
- Kergosien, Y., Ch Lenté, D. Piton, J. C. Billaut. 2011. A tabu search heuristic for the dynamic transportation of patients between care units. *European Journal of Operational Research* **214**(2) 442–452.
- Kim, B.-I., J. Koo, J. Park. 2010. The combined manpower-vehicle routing problem for multi-staged services. *Expert Systems with Applications* **37**(12) 8424–8431.
- Klein, R., A. Scholl. 1999. Computing lower bounds by destructive improvement: An application to resource-constrained project scheduling. *European Journal of Operational Research* **112**(2) 322–346.

- Kliewer, Natalia, Bastian Amberg, Boris Amberg. 2012. Multiple depot vehicle and crew scheduling with time windows for scheduled trips. *Public Transport* **3**(3) 213–244.
- Koubâa, M., S. Dhouib, D. Dhouib, A. El Mhamedi. 2016. Truck Driver Scheduling Problem: Literature Review. *IFAC-PapersOnLine* **49**(12) 1950–1955.
- Lam, E., P. Van Hentenryck, P. Kilby. 2020. Joint Vehicle and Crew Routing and Scheduling. *Transportation Science* **54**(2) 488–511.
- Larrain, H., L. C. Coelho, A. Cataldo. 2017. A Variable MIP Neighborhood Descent algorithm for managing inventory and distribution of cash in automated teller machines. *Computers & Operations Research* **85** 22–31.
- Meisel, F., H. Kopfer. 2014. Synchronized routing of active and passive means of transport. *OR Spectrum* **36**(2) 297–322.
- Schiffer, M., G. Laporte, M. Schneider, G. Walther. 2017. The impact of synchronizing driver breaks and recharging operations for electric vehicles. Tech. Rep. G-2017-46, GERAD, HEC Montreal, Canada.
- Schiffer, M., M. Schneider, G. Walther, G. Laporte. 2019. Vehicle Routing and Location Routing with Intermediate Stops: A Review. *Transportation Science* **53**(2) 319–343.
- Schiffer, M., G. Walther. 2018. An Adaptive Large Neighborhood Search for the Location-routing Problem with Intra-route Facilities. *Transportation Science* **52**(2) 331–352.
- Schneider, M., M. Löffler. 2019. Large Composite Neighborhoods for the Capacitated Location-Routing Problem. *Transportation Science* **53**(1) 301–318.
- Tilk, C., N. Bianchessi, M. Drexl, S. Irnich, F. Meisel. 2018. Branch-and-Price-and-Cut for the Active-Passive Vehicle-Routing Problem. *Transportation Science* **52**(2) 300–319.
- Tilk, C., M. Drexl, S. Irnich. 2019. Nested branch-and-price-and-cut for vehicle routing problems with multiple resource interdependencies. *European Journal of Operational Research* **276**(2) 549–565.
- Tilk, C., A. Goel. 2020. Bidirectional labeling for solving vehicle routing and truck driver scheduling problems. *European Journal of Operational Research* **283**(1) 108–124.
- Yin, Jiateng, Andrea D’Ariano, Yihui Wang, Lixing Yang, Tao Tang. 2021. Timetable coordination in a rail transit network with time-dependent passenger demand. *European Journal of Operational Research* **295**(1) 183–202.

## Appendix A: MIP with Consideration of the Subcontractor's Objectives

To create driver schedules according to the subcontractor's objective with the MIP defined in Section 3.2, we need to modify some constraints and variables. In the following, we describe the modifications needed. Specifically, we consider the following five objective functions: i) minimize the total workload, ii) balance the workload, iii) minimize the total steering time, iv) balance the steering time, v) minimize the total ride duration. Given an optimal driver count  $X^*$  resulting from the solution of the original problem as formalized in Section 3.2, we first fix the number of drivers to this value. We do so by tightening the set of drivers to  $\mathcal{K} = \{1, \dots, X^*\}$ , fixing the lower bound to  $LB = X^*$ , and replacing Constraint (21) with Equality (25):

$$\sum_{k \in \mathcal{K}} \sum_{i \in \mathcal{T}(0)} \sum_{(i,j,m) \in \delta^+(i)} x_{kijm} = LB \quad (25)$$

Next, we can integrate the objective function. To minimize the total workload, we replace objective function (1) with (26):

$$\min \sum_{k \in \mathcal{K}} \left( \sum_{i \in \mathcal{T}(0)} \sum_{(j,i,m) \in \delta^-(i)} t_j x_{kijm} - \sum_{i \in \mathcal{T}(0)} \sum_{(i,j,m) \in \delta^+(i)} t_j x_{kijm} \right) \quad (26)$$

To minimize the total steering time, we replace objective function (1) with (27):

$$\min \sum_{k \in \mathcal{K}} \sum_{\substack{(i,j,m) \in \mathcal{A}: \\ m=1}} c_{ijm} x_{kijm} \quad (27)$$

To minimize the total duration of all bus rides, we replace objective function (1) with (28):

$$\min \sum_{r \in \mathcal{R}} \sum_{k \in \mathcal{K}} \left( \sum_{\substack{(j,i,m) \in \mathcal{A}: \\ i \in \mathcal{T}(d_r), m=1}} t_i x_{kijm} - \sum_{\substack{(i,j,m) \in \mathcal{A}: \\ i \in \mathcal{T}(p_r), m=1}} t_i x_{kijm} \right) \quad (28)$$

To integrate balancing objective functions, we define two additional decision variables  $\bar{b} \geq 0$  and  $\underline{b} \leq 0$ . We also add constraints connecting the balancing variables with the resources to be balanced. For balancing the workload, we replace objective function (1) with (29) and add constraints (30) - (31) and variable domains (32) - (33) to the model:

$$\min \quad \bar{b} + \underline{b} \quad (29)$$

$$\sum_{i \in \mathcal{T}(0)} \sum_{(j,i,m) \in \delta^-(i)} t_j x_{kijm} - \sum_{i \in \mathcal{T}(0)} \sum_{(i,j,m) \in \delta^+(i)} t_j x_{kijm} \leq \bar{b} \quad \forall k \in \mathcal{K} \quad (30)$$

$$-\left( \sum_{i \in \mathcal{T}(0)} \sum_{(j,i,m) \in \delta^-(i)} t_j x_{kijm} - \sum_{i \in \mathcal{T}(0)} \sum_{(i,j,m) \in \delta^+(i)} t_j x_{kijm} \right) \leq \underline{b} \quad \forall k \in \mathcal{K} \quad (31)$$

$$\bar{b} \geq 0 \quad (32)$$

$$\underline{b} \leq 0 \quad (33)$$

To balance the steering time, we use the same objective function (29) and variable domains (32) - (33), but

instead of constraints (30) - (31) we add constraints (34) - (35) to the model:

$$\sum_{\substack{(i,j,m) \in \mathcal{A}: \\ m=1}} c_{ijm} x_{kijm} \leq \bar{b} \quad \forall k \in \mathcal{K} \quad (34)$$

$$- \sum_{\substack{(i,j,m) \in \mathcal{A}: \\ m=1}} c_{ijm} x_{kijm} \leq \underline{b} \quad \forall k \in \mathcal{K} \quad (35)$$

Preliminary experiments showed that the problem complexity and improvement potential vary notably depending on the objective function used. For a 10% subset of all small instances, Table 18 depicts the average computational time to optimality (t[s]), the absolute improvement in minutes compared to the optimal solution of the original problem as defined in Sections 3.2 and 3.3 ( $\Delta z[\text{min}]$ ), and the relative improvement ( $\Delta z[\%]$ ), respectively. As expected, the improvement potential of the total steering time and the total ride duration is below 1% and thus negligible. This is due to the detour limit  $\zeta$ , which allows only minor deviations from the minimum driving times required for a ride. On the other hand, the total workload can be reduced by 17.58% or 247.38 minutes on average. With more than 60%, the improvement potential for balancing objectives is even higher. However, this optimization potential comes at the cost of an increase in computational time by more than a factor of 100 compared to the DRSPMS minimizing the total driver count.

In general, the MIP can solve only small instances and is not tractable for medium or large instances. We leave the development of advanced solution methods for the subcontractors' objectives for future research.

## Appendix B: Computational Analysis of the Lower Bounds

We conducted a computational analysis based on a subset of instances to evaluate the quality of our different constructive lower bounds described in Section 3.3. We computed lower bounds  $LB_1$  and  $LB_2$ , the combination of both ( $LB$ ), and the linear programming relaxation ( $LP$ ) for every instance in our subset. Table 19 shows the share of instances for which one lower bound dominates the other in terms of objective value. Between  $LB_1$  and  $LB_2$ , no approach can be proven to be superior over the other. While bound  $LB_1$  is superior over bound  $LB_2$  for 69.54% of the instances, there also exist instances (1.72%) for which  $LB_2$  is stronger. Furthermore, bound  $LB_1$  outperforms the LP relaxation for 48.94% of the instances. The main weakness of the LP relaxation is that by allowing fractional arc flows, steering times and working times are not increased by the respective arc's full steering or working time but only by a fraction of it. Thus, none of the working and steering time regulations are sufficiently considered in the LP relaxation. Instead,

Table 18: Post-optimization on subcontractor-level

Objective	t[s]	$\Delta z[\text{min}]$	$\Delta z[\%]$
i) Minimize workload	43.35	247.38	17.58
ii) Balance workload	24.55	153.60	65.24
iii) Minimize steering	0.12	1.42	0.17
iv) Balance steering	77.24	75.99	62.01
v) Minimize ride duration	0.18	2.50	0.26

bound  $LB_1$  relaxes mainly the continuous steering time limit. However, bound  $LB_1$  does not consider that a driver can serve only one ride at a time. By combining bound  $LB_1$  with  $LB_2$ , which accounts for the latter, the combined bound  $LB$  dominates the LP relaxation for all instances. Furthermore, the combined bound  $LB$  dominates bounds  $LB_1$  and  $LB_2$  by definition. Therefore, we use the combined lower bound  $LB$  in our algorithmic framework.

### Appendix C: Computational Analysis of the Algorithmic Components

To evaluate the impact of the different components in our solution approach, we run a computational study including 10% of all instances. Specifically, we consider the following five components: the construction heuristic (CH), the LS to improve the constructive start solution (LS), the destructive bound improvement procedure (DBI), callback routines applying the LS to new incumbents (CB), and the MIP (MIP). We tested seven variants, with Variant 0 being the base variant containing all solution components. For Variants 1 to 6, we switched off one component as shown in Table 20. Note that both Variant 5 and Variant 6 exclude the MIP and the CB. For Variant 5, we increase the remaining components’ time limit to the global time limit. In contrast, for Variant 6, we keep the time limits of the remaining components unchanged. For every variant, we conducted 10 runs per instance. Table 20 shows the share of instances solved to feasibility (solved[%]), the share of instances solved to optimality (opt.solved[%]), and the average deviation over 10 runs from the best objective ( $\Delta z$ [%]) and from the best optimality gap ( $\Delta gap$ [%]). The results in Table 20 show that Variant 0 performs best, implying that every component of our solution approach contributes to the solution quality. Removing the DBI, as done in Variant 1, increases the average deviation from the best optimality gap by more than factor six and further increases the objective function value. Due to the lack of a heuristic start solution, Variant 2 fails to find any feasible solution for 10 of 35 instances after 3,600 seconds. Thus,  $\Delta z$  and  $\Delta gap$

Table 19: Comparison of lower bounds

dominates	$LB_1$	$LB_2$	$LB$	$LP$
$LB_1$	-	0.6954	0.000	0.4894
$LB_2$	0.0172	-	0.000	0.000
<b><math>LB</math></b>	<b>0.0172</b>	<b>0.6954</b>	-	<b>0.4894</b>
$LP$	0.0071	0.0426	0.000	-

Table 20: Contribution of the algorithmic components

Components	Variants						
	0	1	2	3	4	5	6
CH	✓	✓		✓	✓	✓	✓
LS	✓	✓			✓	✓	✓
DBI	✓		✓	✓	✓	✓	✓
CB	✓	✓	✓	✓			
MIP	✓	✓	✓	✓	✓		
solved [%]	<b>100.00</b>	100.00	71.43	100.00	100.00	100.00	100.00
opt.solved [%]	<b>60.46</b>	60.17	60.17	59.89	60.17	60.17	57.31
$\Delta z$ [%]	<b>0.05</b>	0.20	-	0.24	1.21	2.16	2.16
$\Delta gap$ [%]	<b>0.51</b>	3.18	-	0.82	1.74	1.98	3.86

cannot be determined. By including the CH, feasible solutions can be generated for all instances. However, without the local search component as in Variant 3, the obtained objective values and the obtained optimality gaps for instances not solved optimally suffer. Removing CB, as in Variant 4, reduces the quality of obtained solutions, particularly for instances not solved optimally. Interestingly, removing the MIP component does not impact the share of instances solved to optimality any further if the remaining components' time limit is increased as in Variant 5. Without extending the time limit, however, the share of instances solved to optimality decreases by 4.75%, see Variant 6. In any case, the objective function value and the gap increase.

## Appendix D: Computational Analysis of Neighborhood Search Variants

We implemented and compared two different search structures: a standard variable neighborhood descent (VND), applying all operators defined in Section 3.4.4 sequentially, and a LS (LS), exploring the same operators in a composite setting as outlined in Section 3.4.4. To compare both neighborhood structures, we run a computational study on a subset including 10% of all instances presented in Section 4.1. Table 21 shows the average deviation of the objective value ( $\Delta z[\%]$ ), the gap ( $\Delta gap[\%]$ ), and the computational time ( $\Delta t[\%]$ ) from best-known values grouped by instance size. The results in Table 21 indicate only minor performance differences between the two neighborhood structures. The composite-neighborhood-based LS meets all best-known values in terms of objective value and gap. In contrast, results obtained by the VND deviate by 0.36% and 0.48% from the best-known values for large instances. Due to the more aggressive search behavior, the LS outperforms the VND in terms of computational time for small- and medium-sized instances. However, the VND structure results in shorter computational times for large instances. As we restrict computational times for all runs, we are mainly interested in the approach that results in the best objective value. Thus, we chose the composite setting in the local search phase of our matheuristic.

Table 21: Performance of different neighborhood structures

Instance size	VND			LS		
	$\Delta z[\%]$	$\Delta gap[\%]$	$\Delta t[\%]$	$\Delta z[\%]$	$\Delta gap[\%]$	$\Delta t[\%]$
Small	0.00	0.00	50.92	0.00	0.00	3.85
Medium	0.00	0.00	27.33	0.00	0.00	16.41
Large	0.36	0.48	0.01	0.00	0.00	0.15
All	0.09	0.12	27.70	0.00	0.00	8.72